

1 **Abstract**

2

3 NASA's MODerate-resolution Imaging Spectroradiometers (MODIS) have been
4 observing the Earth from polar orbit, from *Terra* since early 2000 and from *Aqua* since
5 mid 2002. We have applied a consistent retrieval and processing algorithm to the entire
6 time series of both MODISs, deriving the Collection 5 (C005) dark-target aerosol
7 products. Here, we co-locate the MODIS field of view aerosol retrievals (Level 2) with
8 AERONET sunphotometer measurements at nearly 300 sites, resulting in over 100,000
9 matched pairs. Over land and ocean separately, we characterize the expected uncertainty
10 (EU) for particular MODIS -derived aerosol parameters. We demonstrate that global EU
11 for total and spectral aerosol optical depth (AOD or τ) is $\pm(0.05+0.15\tau)$ and
12 $\pm(0.04+0.05\tau)$ over dark land and ocean respectively. We identify systematic errors at
13 particular sites and seasons. In some cases AOD agreement is good at all wavelengths, in
14 others the AOD is accurate at one wavelength, but spectral dependencies are not well
15 captured. For yet others, AOD in all wavelengths compares poorly. We also assess
16 MODIS-derived aerosol size parameters. With EU of ± 0.45 , MODIS has little skill at
17 deriving Ångström exponent (α) over land, globally, but has qualitative accuracy over
18 specific sites. Over the global ocean, α is much better constrained (EU = ± 0.3), although
19 there are clear biases for regions known for dust or higher aerosol absorption. A better
20 alternative for estimating submicron-sized aerosol contribution is the fine aerosol AOD
21 (fAOD), which is shown to have EU over land and ocean more similar to the total AOD.
22 Finally, we define the Fraction of EU (FEU) for AOD, to characterize how the sensors
23 may be changing over time. We find that the MODIS/AERONET comparison is

24 consistent throughout the entire mission for both Terra and Aqua over ocean, as well as
25 for Aqua over land. There is a systematic change for Terra over land that we believe to be
26 a result of calibration uncertainty.

27

28 **1. Introduction**

29

30 As components in Earth's global climate system, characterizing aerosols' global
31 distribution and loading are necessary for understanding their impacts. The climate and
32 aerosol communities are increasingly relying on satellite-derived aerosol data, including
33 products of passive remote sensing. Aerosol products from NASA's Moderate Imaging
34 Spectrometer (MODIS) sensor were utilized in the latest IPCC (4th) assessment of climate
35 [IPCC, 2007]. Satellite aerosol products, including those from MODIS, are also being
36 used for estimating and monitoring ground-level particulate matter (PM) at regional and
37 local scales [e.g., *Al-Saadi et al.*, 2005].

38

39 There are two MODIS sensors, observing Earth from polar orbit (705 km altitude) aboard
40 NASA's *Terra* (since Feb 2000) and *Aqua* satellites (since June 2002). MODIS has an
41 attractive combination of swath size (~2330 km), spectral resolution (36 wavelength
42 bands, spanning from 0.415 μm to 14.5 μm) and spatial resolution (1 km, 0.5 km, or 0.25
43 km, depending on band). For each instrument, spatial and spectral performance has been
44 monitored and maintained by the MODIS Characterization Support Team (MCST), such
45 that for typical situations, calibration error is within $\pm 2\text{-}3\%$. Thus, MODIS has
46 contributed over nine years of comprehensive, stable and dependable observations of

47 Earth's spectral radiance. The MODIS aerosol algorithm relies on these optimal
48 observations, ensuring long term accuracy, stability and usefulness of the retrieved
49 aerosol products.
50
51 To take advantage of MODIS's sensitivity to aerosol signals, efficient and accurate
52 retrieval algorithms have been developed, maintained, and consistently applied to the
53 observations. Generally, the algorithms operate by matching observed spectral
54 reflectance (statistics of non-cloudy pixels) to lookup tables (LUT) that simulate spectral
55 reflectance for expected aerosol conditions. Each retrieved value represents the aerosol
56 conditions in non-cloudy skies, within some expected uncertainty. The current suite of
57 MODIS aerosol products are derived by separate algorithms that retrieve aerosol
58 properties over three separate environments: 1) dark-surface (far from sun glint) ocean
59 targets [Remer *et al.*, 2005], 2) dark-surface (vegetation and bare soils) land targets [Levy
60 *et al.*, 2007b], and 3) bright surface (deserts) land targets [Hsu *et al.*, 2004]. In this paper,
61 we assess the performance of the aerosol products over the dark-targets (environments 1
62 and 2), where MODIS retrieves total *aerosol optical depth* (*AOD* or τ) at 0.55 μm , as
63 well as other wavelengths in the visible (VIS) and Near-IR (NIR) spectrum. The dark
64 target algorithms are also designed to retrieve some characteristics of submicron-sized
65 aerosols (having radius less than approximately 1.0 μm). These size products include the
66 *fine aerosol fraction* (*FF* or η), the *Ångström exponent* (α) and the *fine mode AOD*
67 (*fAOD* or τ_f). Retrievals of the total AOD and size parameters, including diagnostic
68 parameters and retrieval *Quality Assurance* (*QA*), comprise the set of *Level 2 (L2)* aerosol
69 products. These L2 products are retrieved at 10 km resolution globally, and are processed

70 by the MODIS Adaptive Processing System (MODAPS) at NASA's Goddard Space
71 Flight Center. The most recent data (known as Collection 5, or C005) are freely available
72 via the MODAPS web site.

73

74 The last comprehensive evaluation of regional and global MODIS aerosol products was
75 performed for Collection 4 (C004) [Remer *et al.*, 2005]. Since then, the over land portion
76 of the algorithm received a complete overhaul, (Levy *et al.*, 2007a, 2007b) whereas the
77 over-ocean portion was more conservatively updated (Remer *et al.*, 2006). The Deep
78 Blue algorithm [e.g., Hsu *et al.*, 2004] was added for bright surfaces, but its products are
79 available for only a subset of Aqua data. A detailed global evaluation of Deep Blue
80 products requires a separate paper, so it is not presented here. Although there has been
81 some evaluation of C005 dark-target products both globally [e.g. Remer *et al.*, 2008], and
82 regionally [e.g. Mi *et al.*, 2007], these references do not perform the in depth study we
83 show here. Here, we “validate” total spectral AOD as well as particular aerosol size
84 products, globally, regionally, and seasonally. We quantify the expected uncertainty (EU)
85 of the MODIS products, by comparing with similar parameters derived from the sun/sky
86 radiometers of the global Aerosol Robotic Network (AERONET, [Holben *et al.*, 1998]).

87

88 In Section 2, we briefly introduce the recent changes to the dark-target aerosol retrieval
89 and products that are relevant for C005, and define the concept of “validation.” We
90 compare the MODIS –derived aerosol products to measurements by ground-based
91 sunphotometers, for spectral AOD in Section 3, and for aerosol size parameters
92 (including Ångström exponent and fine AOD) in Section 4. We use the spatial-temporal

93 collocation method that was introduced by *Ichoku et al.*, [2002], and used previously by
94 *Remer et al.*, [2005] and others. In section 5, we summarize our validation results and
95 suggest steps necessary to reduce systematic discrepancies. Section 6 offers some
96 discussion of the significance of the results and conclusions.

97

98 **2. The MODIS aerosol retrieval**

99

100 The MODIS dark-target aerosol retrieval uses portions of the visible (VIS), near-IR
101 (NIR), and shortwave IR (SWIR) spectrum, specifically two 250 m resolution bands
102 (centered about 0.66 and 0.86 μm), and five 500 m resolution bands (centered about 0.47,
103 0.55, 1.2, 1.6 and 2.1 μm). These bands are all in gas-absorption window regions, so that
104 when constrained properly, they provide a clear signal of aerosol effects in atmospheric
105 radiative transfer. The algorithm uses additional wavelengths in other parts of the
106 spectrum to identify and mask out clouds and suspended river sediments [*Ackerman et*
107 *al.*, 1998, *Gao et al.*, 2002; *Martins et al.*, 2002; *Li et al.*, 2003]. Based on studies of
108 MODIS's spectral signal-to-noise properties, and the relationships of surface and aerosol
109 optical properties, MODIS is capable of retrieving global aerosol properties at 10 km x
110 10 km resolution [e.g. *Levy et al.*, 2009b]. Both aerosol algorithms utilize pre-computed
111 lookup tables (LUT) that simulate spectral reflectance from a number of probable aerosol
112 scenarios.

113

114 By assuming properties of the surface reflectance, each dark-target algorithm uses the
115 LUT to determine which aerosol scenario best “matches” the observations of spectral

116 reflectance. Although the mechanisms of each algorithm are different, their solutions
 117 include a measure of total aerosol loading known as the aerosol optical depth (AOD, or τ)
 118 and a measure of the fraction of the optical depth attributed to fine-sized particles, known
 119 as the fine aerosol fraction (FF or η). Total AOD is a straightforward measure of
 120 column-integrated extinction, and is directly retrieved at 0.55 μm . Over the ocean, where
 121 the algorithm combines lognormal modes, the FF is the fraction of the AOD contributed
 122 by the fine-mode (aerosol modes with effective radius less than 1.0 μm). Over land,
 123 where bi-lognormal models take the place of single modes in the algorithm, the FF is the
 124 fraction of the AOD contributed by the fine-dominated model. Because the FF is defined
 125 differently over land and ocean, and is defined differently by AERONET [O'Neill *et al.*,
 126 2003; Kleidman *et al.*, 2005], it is very difficult to evaluate. Instead, we look to the
 127 combination of AOD and FF, plus knowledge of which modes (ocean) or models (land)
 128 were used for the solution, to lead to aerosol size parameters that are easier to compare
 129 and evaluate. We define the spectral AOD, Ångström exponent (α), and fine AOD
 130 (fAOD or τ_F) below.

131
 132 The MODIS algorithm derives AOD in all seven channels (0.47-2.12 μm) over ocean and
 133 at the three VIS channels over land (0.47, 0.55, and 0.66 μm). The *Ångström exponent*
 134 (α) describes the spectral dependence of the AOD in natural log space, and is a proxy for
 135 aerosol size distribution [e.g. Eck *et al.*, 1999]. It is defined in its simplest form as

$$136 \quad \alpha_{\lambda_1, \lambda_2} = -\frac{\ln(\tau_{\lambda_1}/\tau_{\lambda_2})}{\ln(\lambda_1/\lambda_2)}, \quad (1)$$

137 where λ_1 and λ_2 are any two wavelengths, usually in the visible or near IR spectrum.
138 Larger Ångström exponent values indicate dominance of smaller particles, and vice
139 versa. The combination of wavelengths is defined differently over ocean and land. Over
140 ocean, MODIS derives two Ångström exponents, one derived from 0.55 μm / 0.86 μm
141 ($\alpha_{o,1}$), and the other from 0.86 μm / 2.1 μm ($\alpha_{o,2}$). The use of two values across this
142 wavelength range help to detect spectral curvature, and aid in differentiating particle sizes
143 and types [Eck *et al.*, 1999]. However, since AERONET does not measure far into the
144 SWIR, for this paper, we compare only the values for $\alpha_o = \alpha_{o,1}$. Over land, only one value
145 is derived, for 0.47 μm / 0.66 μm and is denoted as α_L .

146

147 Since the FF is difficult to evaluate (differences in definitions) and quantify (unstable to
148 inputs and assumptions; e.g. [Levy *et al.*, 2007b]) we shall calculate the fine aerosol
149 optical depth (fAOD) by multiplying FF and AOD (i.e., $\tau_F = \eta\tau$), defined at 0.55 μm .
150 The fAOD represents the aerosol optical depth attributed to fine-sized particles, and
151 should be less sensitive to whether fine refers to “fine-mode” (over ocean) or “fine-
152 dominated model” (over land). Since fine-sized (accumulation mode) particles often
153 originate from anthropogenic combustion processes, such as urban pollution or biomass
154 burning. The fAOD can help to identify aerosols of anthropogenic origin, even if fAOD
155 is not the same as anthropogenic AOD [e.g. Kaufman *et al.*, 2003].

156

157 In addition to retrieving the spectral AOD and several aerosol size parameters, the
158 algorithm assesses the confidence of a given retrieval, using a logic known as the *Quality*
159 *Assurance (QA)* plan. Quality Assurance represents a series of tests that are applied

160 during the retrieval process, in order to characterize the expected confidence of the
161 retrieved product. QA assesses the quality and confidence of the input MODIS
162 reflectance data, ancillary datasets [e.g. meteorology or ozone ancillary data; *Levy et al.*,
163 2009b], and/or output products. For example, one might ask, “after cloud screening and
164 data selection, how many pixels are left to make a retrieval?” Given two retrievals of the
165 same AOD, a solution that utilized more pixels may be expected to have higher
166 confidence than one made from fewer pixels. Or one may ask, “How well does the best
167 aerosol solution fit to the observed spectral reflectance?” A poor fit could be cause for
168 lower confidence in the solution, and the QA would be adjusted accordingly. At the
169 conclusion of the entire retrieval process, a final summary *Quality Confidence (QC)* flag
170 is assigned to represent the aggregation of the QA tests. QC ranges from 0 to 3, indicating
171 low, marginal, medium or high confidence in the solution. While the QC has no inherent
172 relationship to whether a given MODIS AOD is comparable to a given AERONET AOD,
173 higher confidence solutions tend to show better agreement. Thus, we limit our validation
174 exercise to the best data only, which is defined in the later sections.

175

176 **2.1 The MODIS aerosol algorithm through Collection 4**

177

178 The MODIS dark-target retrieval concept was conceived prior to *Terra* launch, based on
179 *Kaufman et al.*, [1997] over land, and *Tanré et al.*, [1996; 1997] over ocean. Their
180 versions of the algorithms were implemented at first light and have evolved continuously,
181 based on acquiring new scientific knowledge as well as new processing needs. Based on
182 groupings of similar algorithms and data processing, there have been have been sets of

183 products, known as “Collections”. Early evaluation of Collection 2 and 3 MODIS
184 products [e.g. *Chu et al., 2002; Remer et al., 2002*], showed remarkable agreement in
185 retrieved AOD, but also suggested how the algorithms could be improved. The last
186 comprehensive global evaluation was performed for Collection 4 (C004) [*Remer et al.,*
187 2005].

188

189 The C004 evaluation [*Remer et al., 2005*] compared MODIS L2 AOD products (10 km x
190 10 km resolution) with measurements from 132 globally distributed ground stations of
191 the Aerosol Robotic Network (AERONET; *Holben et al., 1998*). This paper “validated”
192 the MODIS-derived spectral AOD, meaning that one standard deviation (~66%) of the
193 MODIS points fell within some expected uncertainty (*EU*) interval of the ground truth
194 measurements. The EU for AOD (τ_{EU}) was defined as

$$195 \quad \tau_{EU} = \pm(A + B\tau), \quad (2)$$

196 where A and B are coefficients, and $\tau = \tau_{AERONET}$ (AOD measured by AERONET). These
197 EU were previously defined as $\tau_{EU} = \pm(0.03 + 0.05\tau)$ over ocean [*Remer et al., 2002*] and
198 $\tau_{EU} = \pm(0.05 + 0.15\tau)$ over land [*Chu et al., 2002*]. Although the paper concluded that the
199 MODIS total and spectral AOD could be considered validated, certain systematic biases
200 were also noted. Over ocean, there was minor under-prediction of high AOD (slope =
201 0.94 at 0.55 μm), which was more significant for land (slope = 0.78). Over ocean,
202 retrieval of low AOD was generally quantitative as demonstrated by the minimal y-offset
203 (+0.005). There was, however, a significant offset over land (+0.068).

204

205 *Remer et al.*, [2005] also evaluated some aspects of the global aerosol size retrievals in
206 C004. Over land, they indicated that averages of retrieved FF might be reasonable, but
207 that scatter plots (not shown in their paper) suggested little or no skill at retrieving FF in a
208 given scene. Over ocean, although they found a general underestimation of FF, it was
209 often overestimated in heavy dust loadings. They also found that the FF retrieval over
210 ocean could be heavily impacted by calibration. Further study by *Kleidman et al.* [2005]
211 showed that FF could be even more significantly underestimated in conditions of heavy
212 smoke or pollution loadings, and confirmed the overestimate (by 0.1-0.2) in dusty scenes.
213 In another study, however, which compared MODIS data to airborne sunphotometer
214 measurements, MODIS overestimated FF by 0.2 even when dust was not observed
215 [*Anderson et al.*, 2005].

216

217 In addition to the conclusions of *Remer et al.*, [2005] for global data, there were a number
218 of regional studies (e.g. [*Levy et al.*, 2005; *Jethva et al.*, 2007a; *Mi et al.*, 2007] that
219 demonstrated that the total AOD over-land was even more significantly biased in certain
220 regions. Also, since the retrieval of FF was essentially meaningless over land, it became
221 apparent that a complete overhaul of the over-land algorithm was necessary. Over ocean,
222 while there was little bias in the total AOD retrieval, there was still the offset in derived
223 spectral dependence and FF (e.g. *Remer et al.*, [2005], *Kleidman et al.*, [2005] and
224 *Anderson et al.*, [2005]) to consider. Therefore, refinements were also proposed for the
225 over-ocean algorithm.

226

227 An unexpected problem with the C004 processing effort was that both the aerosol
228 retrieval algorithm and the input radiances were allowed to evolve all using the C004
229 label. It was known that the aerosol algorithm was sensitive to the instrument calibration
230 [e.g. *Tanré et al.*, 1997; *Levy et al.*, 2007], as well as to upstream products (e.g., cloud
231 mask, water vapor retrieval). However, during the processing of the C004 MODIS
232 aerosol algorithm, the upstream products and the calibration coefficients both underwent
233 refinements (bug fixes, lookup table coefficients, etc) during the lifetime of the
234 Collection. This meant that the combination of “forward” processing in real time (from
235 2004 onward) and “re-processing” of archived data (prior to 2004) was not performed
236 consistently. Although in most cases these changes did not significantly impact the
237 results, detailed analysis of certain data products showed trends or spikes associated with
238 one or more of the changes. Thus, it was clear that it was necessary to reprocess the entire
239 MODIS mission, using consistent calibration coefficients, upstream algorithms and
240 aerosol retrieval. MODAPS began both forward processing and re-processing in early
241 2006, thus deriving the C005 aerosol products evaluated in this paper. A summary of the
242 aerosol retrieval process is in the following subsections.

243

244 **2.2 Collection 5 land algorithm**

245

246 Based on the global and regional assessments of C004 (and prior) aerosol products over
247 land, it was seen that while mostly within expected uncertainty, there was a tendency for
248 biases both in low and high AOD conditions. *Levy et al.*, [2005] studied both offset and
249 slope issues over land, and concluded that a combination of refined surface reflectance

250 assumptions and aerosol optical assumptions could help to reduce biases in specific
251 regions or seasons. Some errors could also be pegged to the neglect of polarization in the
252 C004 radiative transfer calculations [Levy *et al.*, 2004]. As a result, the “second-
253 generation” algorithm was developed [Levy *et al.*, 2007a; 2007b; Remer *et al.*, 2006], and
254 was implemented operationally in early 2006 to derive the C005 products.

255

256 Essentially, the second-generation algorithm over land was a complete overhaul. All
257 assumptions about aerosol optical properties were modified [Levy *et al.*, 2007b], as were
258 surface assumptions [Levy *et al.*, 2007b] and snow masking [Li *et al.*, 2003]. To reduce
259 statistical biases in clean aerosol ($\tau < 0.05$) conditions, small negative AOD values were
260 permitted, archived and assigned a high QC rating. Furthermore, the treatment of
261 Rayleigh/aerosol interaction over elevated targets was changed. A vector radiative
262 transfer code replaced the scalar code used in Collection 4, and the overall inversion
263 scheme was changed to reflect the possibility of dust aerosol signal in the SWIR
264 wavelength region. Using a substantial test-bed of C004 radiance data [Levy *et al.*,
265 2007a], the overall mean AOD of the test-bed retrievals went from ~ 0.28 (using the C004
266 algorithm) to ~ 0.19 (using the C005 algorithm). Comparison of total AOD with
267 AERONET measurements (> 1200 cases) was improved significantly, as demonstrated by
268 higher correlation (R increasing from 0.847 to 0.894), and smaller y-offset (from 0.097 to
269 0.029). Nearly 67% of MODIS AOD retrievals compared to AERONET within the EU
270 of $\pm(0.15 + 0.05\tau)$, indicating that the C005 algorithm could be validated, at least for the
271 test-bed. Furthermore, there were minor improvements observed for retrievals of FF,
272 Ångström exponent, and fAOD over land, using the new algorithm [Levy *et al.*, 2007a].

273

274 In addition to revised assumptions and mathematical fitting, the second-generation
275 algorithm also included major changes to its Quality Assurance (QA) plan. Explanation
276 of the QA tests and assigned QC summary flags can be found in *Levy et al.*, [2009b].
277 Depending on which tests pass or fail, the algorithm may report non-fill (missing) values
278 for all, none or some of the parameters. For example, if the retrieved AOD is less than
279 0.2, the derived fAOD value will be reported, but not the FF. If retrieved AOD is
280 reported but negative (e.g. > -0.05), then neither fAOD nor FF have meaning, and both
281 would be reported as fill-value. Thus, there are fewer pixels with FF and fAOD reported
282 than for total AOD. Yet, if all other QA tests pass, then the reported small AOD value
283 may still receive high confidence (i.e., QC=3). While the QC has no inherent relationship
284 to whether a given MODIS AOD is comparable to a given AERONET AOD, we find that
285 data with QC<3 do not compare well. Therefore, for this work, we limit our validation
286 effort to the set of high confidence (QC=3) data, about 60% of the reported (non-fill
287 value) AOD retrievals [*Levy et al.*, 2009a].

288

289 **2.2 Collection 5 ocean algorithm**

290

291 Between C004 and C005, the only difference in the over-ocean algorithm was an
292 adjustment to sea-salt aerosol refractive index, that better matches more recent
293 observations [*Remer et al.*, 2006]. Although there were large error bars reported,
294 AERONET retrievals of aerosol optical properties over ocean (available only after Terra-
295 MODIS launch) suggested that the real part of the refractive index for sea salt was

296 smaller than the 1.43 used for C004, and more like 1.35 (*Dubovik et al.*, [2002]). Using a
297 test-bed of C004 radiance data [e.g. *Remer et al.*, 2006], and applying the reduced real
298 part of the refractive index, it was found that much of the FF bias observed by *Kleidman*
299 *et al.*, [2005] could be removed without impacting the total AOD retrieval. The mean
300 AOD using either software remained at 0.15, but mean FF was reduced from 0.47 to 0.39.
301 Comparison of MODIS with AERONET for 162 collocations demonstrated that retrieval
302 of AOD was unchanged but that correlation (R), slope, and y-intercept were all improved
303 for retrievals of FF [*Remer et al.*, 2006]. Thus, based on our preliminary study, compared
304 to the C004 algorithm we expected C005 to report smaller fine fraction without changing
305 the statistics of the total AOD.

306

307 Analogous to that described for over land, there is a QA plan for assessing retrieval
308 confidence over ocean [*Levy et al.*, 2009b]. Like over land, the QA logic derives a final
309 QC value for each retrieved 10 km x 10 km pixel, ranging from 0 (low confidence) to 3
310 (high confidence). Certain tests are stricter for ocean than for land, such that only 25% of
311 the pixels over ocean receive QC=3 [*Levy et al.*, 2009a]. However, preliminary efforts
312 showed that even “marginal” confidence data (i.e. QC=1) compared well with
313 AERONET. Thus, for this paper, we have included all ocean data with $QC \geq 1$, thereby
314 including 98% of the reported (non-fill) AOD values over ocean.

315

316 **2.4 Notes on collection 5 products**

317

318 Although the preliminary testing of the C005 algorithms [*Levy et al., 2007a; Remer et al.,*
319 2006] showed improvements over the C004 algorithm, the exercise was based on using a
320 database of archived reflectance data. While there were many MODIS/AERONET
321 collocations (nearly 1400 combined over land and ocean), the test bed was limited in time
322 and space. Furthermore, this test bed was made up of archived C004 reflectance data.
323 However, when C005 was actually processed (and re-processed for data prior to 2006),
324 the MCST introduced revised calibration coefficients. Thus, actual C005 input
325 reflectances are different from the C005-like inputs of the test-bed. When we compare
326 our products to AERONET data, we are testing both the validity of the new algorithms,
327 as well as the validity of the C005 calibration.

328

329 In a recent paper, *Remer et al., [2008]* found that in fact, the products derived from the
330 C005 calibration differed significantly from those that might have been produced via the
331 C004 calibration. Whereas the time series of global monthly AOD values over ocean
332 were nearly exactly the same for Terra and Aqua for C004 [*Remer et al. 2006*], and were
333 not expected (based on the test-bed) to change for C005, analysis of actual C005 data
334 showed that Terra's global monthly mean AOD had increased by nearly 0.015. This
335 increase was seen in all months, including the months prior to 2006 that were
336 reprocessed. Aqua data products did not seem to be affected by revised calibration
337 coefficients. Over land, although *Remer et al., [2008]* noted difficulties in separating
338 calibration and algorithm effects, it is clear that the products were impacted by the
339 revised calibration.

340

341 **3. Comparison of total AOD**

342

343 *Remer et al.*, [2008] began the process of validating the C005 aerosol products, using
344 collocated AERONET data. Their purpose was to ensure that the MODIS products were
345 trustworthy enough to begin to characterize global AOD climatology from the monthly
346 products. In this paper, we concentrate on detailed study of the MODIS L2 products,
347 compared to AERONET, over both land and ocean, and for individual sites. Our purpose
348 is to show where the C005 algorithm works and where it does not.

349

350 Here, we collocate MODIS data with the AERONET Version 2.0, Level 2 Quality
351 Assured (cloud screened and calibrated) sun measurements of spectral AOD
352 [http://aeronet.gsfc.nasa.gov/new_web/Documents/version2_table.pdf] that have 0.01-
353 0.02 uncertainties for all wavelength bands. Using quadratic fits on a log-log scale (e.g.,
354 *Eck et al.*, 1999)), we interpolate the AERONET data to exact MODIS wavelengths (i.e.,
355 0.466, 0.553, 0.644, and 0.865 μm ; [*Remer et al.*, 2006]). We use the spectral de-
356 convolution technique of *O'Neill et al.*, [2003] to derive estimates of FF and fAOD. We
357 employ the spatio-temporal technique of *Ichoku et al.*, [2002], which creates a grid of 5
358 by 5 aerosol MODIS retrievals, with the AERONET station inside the middle pixel.
359 Since each MODIS aerosol pixel represents approximately a 10 km area, the subsetted
360 area is approximately 50 km by 50 km. The spatial statistics of the MODIS retrievals in
361 the 5 by 5 subset are calculated and compared to the temporal statistics of the AERONET
362 observations taken ± 30 minutes of MODIS overpass. At least 5 of the possible 25
363 MODIS retrievals, and 2 of the possible 4 or 5 AERONET observations are required to

364 include the collocation in our statistics. This means that the collocation may not include
365 the exact 10 km MODIS aerosol retrieval in which the AERONET station resides, and
366 could include retrievals from pixels that are 20-25 km away. Although all AERONET
367 sites are land-based (i.e. on continents, on coasts or on islands in ocean basins),
368 assumption of aerosol spatial homogeneity over 50 km (e.g. *Anderson et al.*, [2003])
369 allows us to assess over-ocean aerosol products as well. Using this technique, a coastal
370 AERONET site can be used simultaneously as ground-truth for both land and ocean
371 MODIS aerosol retrievals. It is pertinent to note that for a valid match, both MODIS and
372 AERONET must view conditions sufficiently free of clouds.

373

374 As of September 2008, our database includes collocations over 328 AERONET sites. 203
375 sites are inland, and used exclusively for comparison with the MODIS land products,
376 whereas 32 are island sites used exclusively for over ocean. The rest are located on land
377 near the shoreline so that they can be used for both comparisons. Some sites have been
378 nearly “permanent” and offer a long time series of measurements, whereas other sites
379 may only have measured during a particular season or field experiment. The result is
380 57,796 (39,994) matches for Terra (Aqua) over land and 14,817 (11,392) matches for
381 Terra (Aqua) over ocean. We filter for recommended QC (QC=3 over land; $QC \geq 1$ over
382 ocean), and remove the locations where the elevation of the AERONET site does not
383 represent the surrounding scene. For example, Mauna Loa (elevation 3397 m) should not
384 be used to evaluate aerosol properties over the nearby ocean (elevation 0 m). If the
385 elevations of the AERONET site and the average of the 50 km x 50 km region
386 surrounding it are different by >300 m, then the site is excluded. This also means that

387 coastal AERONET sites may be excluded from comparison with ocean pixels. Still, after
388 QC and elevation filtering, we are left with 35,753 (22,773) collocations for Terra (Aqua)
389 over land and 13,733 (10,407) over ocean.

390

391 3.1 Total AOD over land

392

393 Fig. 1 displays the results of the collocation (filtered for QC=3 and elevation differences
394 less than 300 m), for total AOD (at 0.55 μm) over land, for Terra (left) and Aqua (right).
395 This is a density scatterplot, such that the color of each ordered pair (0.025 x 0.025
396 increment) represents the number of such matchups. The dashed, dotted and solid lines
397 are the 1-1 line, defined EU for land AOD ($\tau_{\text{EU}} = \pm(0.05+0.15\tau)$), and the linear
398 regression of the pre-sorted scatterplot, respectively. Also given for each plot are number
399 of collocations (N), the percent within EU, the regression curve, correlation (R), and the
400 RMS error of the fit. The plots show the quality of the matching, as both Terra and Aqua
401 regressions hug the 1-1 line, have slopes near 1, y-intercepts near zero, and $R>0.9$. One
402 can also see the relative dominance of AOD < 0.25 , with decreasing numbers of points
403 towards the axes limits. Table 1 provides the comparisons for all three wavelengths,
404 including the means of the AOD from both MODIS and AERONET. There is little
405 statistical difference between the overall fits of Terra and Aqua. For both instruments, at
406 least 72% of the points lie within the dotted EU lines (at 0.55 μm), and at least 69% at the
407 other two channels. This suggests that total AOD over land can be considered a
408 “validated” quantity, at least globally within the EU defined by

409

$$\tau_{\text{EU}} = \pm(0.05 + 0.15\tau). \quad (3)$$

Lorraine Remer 3/24/09 7:27 AM

Comment: Do you know why the sharp cut-off at AOD ~ 0.03 in both MODIS and AERONET?

410 **Table 1: Statistics of the comparison between MODIS (Terra and Aqua) and**
 411 **AERONET total spectral AOD over land. The number of points (N) is 35,753**
 412 **(22,773) for Terra (Aqua).**

Sat	Wave (μm)	Mean AOD AERO	Mean AOD MODIS	Regression equation	R	RMS	% in A
Terra	0.47	0.165	0.171	$y = 0.984x + 0.001$	0.892	0.097	74.40
Terra	0.55	0.201	0.202	$y = 0.987x + -0.003$	0.909	0.105	73.01
Terra	0.66	0.250	0.244	$y = 0.985x + -0.009$	0.920	0.120	70.46
Aqua	0.47	0.161	0.164	$y = 0.986x + -0.002$	0.883	0.099	73.55
Aqua	0.55	0.195	0.193	$y = 0.992x + -0.007$	0.898	0.108	71.96
Aqua	0.66	0.242	0.233	$y = 0.991x + -0.013$	0.908	0.123	69.17

413 A: $\text{EU} = \tau_{\text{EU}} = \pm(0.05+0.15\tau)$

414

415 However, global scatterplots like Fig. 1 can hide details. MODIS data may have
 416 systematic biases due to specific conditions (e.g., unique aerosol type, or surface
 417 conditions) encountered at certain sites or during certain seasons. Some sites may be
 418 biased high and others low, and will cancel each other in the global scatterplot. Given our
 419 expected uncertainty of the total AOD at 0.55 μm , we would like to characterize how
 420 well the algorithm is performing at a given site, for a given season. For example, if the
 421 statistics of the AOD comparison shows that MODIS and AERONET are well matched
 422 (66% within EU interval), we might call this a good comparison at the site. If they do not
 423 match, say less than 50% within the EU interval, then this is a poor comparison. We can
 424 extend these conditions to describing the comparison of the total AOD for the other VIS
 425 wavelengths (i.e., 0.47 and 0.66 μm). A condition of retrieving reasonable estimates of
 426 the aerosol size parameters is reasonable characterization of the AOD spectral
 427 dependence. If all channels match within EU, then we can consider it a good all around
 428 comparison. Likewise if all do not match, then this is a poor comparison. However, there
 429 are sites or seasons where the AOD at 0.55 μm compares well, but AOD at one or more
 430 of the other channels do not, or vice versa.

431

432 Fig. 2 provides a color wheel for subjective characterization of matching quality. Each
433 color represents measures of two semi-independent MODIS/AERONET comparison tests
434 (A and B), for a given MODIS-derived parameter. The first test quantifies the number of
435 matched pairs that fit within a defined measure of EU. These matched pairs are assumed
436 to be for the nominal product (e.g., at 0.55 μm for the MODIS AOD product). The
437 second test may refer to a comparison at other wavelengths (for the AOD product) or a
438 different measure entirely (e.g., correlation coefficients instead of number of matched
439 pairs). Table 2 lists the details of comparison tests A and B for a different MODIS
440 derived parameters, and the results that are associated with a given color.

441

442 For example, Fig. 2 may be used to qualify the degree of comparison for the MODIS total
443 AOD product over land, for a given site, for a given season. Test A computes the number
444 of matched pairs (at 0.55 μm) that fall within a defined estimate of EU. Test B computes
445 the number of matched pairs at other channels (0.47 and 0.66 μm) that fall within EU.
446 When referring to total AOD over land, green color (at the top) represents collocations
447 where >66% of the MODIS-derived in all three VIS channels match AOD from
448 AERONET within EU. Red color (at the bottom) represents the condition of <50% match
449 for all three channels. Going counterclockwise (through cold colors) represent cases
450 where the 0.55 μm values continue to match, but less match to one or more of the other
451 VIS channels. Going clockwise (warm colors) represent increasing mismatch at 0.55 μm ,
452 but possibly better comparison at one or more of the other channels.

453 **Table 2: Conditions A and B to designate symbol color for different MODIS**
454 **parameters.**

Color	AOD ocean ¹	AOD land ²	fAOD ocean ³ / land ⁴
Green	$\tau_{0.55}\% \geq 66$ $\tau_{0.87}\% \geq 66$	$\tau_{0.55}\% \geq 66$ $\tau_{0.47}\% \geq 66$ and $\tau_{0.67}\% \geq 66$	$\tau_F\% \geq 66$ $R \geq 0.8$
Cyan	$\tau_{0.55}\% \geq 66$ $50 \leq \tau_{0.87}\% < 66$	$\tau_{0.55}\% \geq 66$ $\tau_{0.47}\% \geq 50$ and $\tau_{0.67}\% \geq 50$	$\tau_F\% \geq 66$ $0.4 \leq R < 0.8$
Blue	$\tau_{0.55}\% \geq 66$ $\tau_{0.87}\% < 50$	$\tau_{0.55}\% \geq 66$ $\tau_{0.47}\% < 50$ or $\tau_{0.67}\% < 50$	$\tau_F\% \geq 66$ $R < 0.4$
Purple	$50 \leq \tau_{0.55}\% < 66$ $\tau_{0.87}\% < 50$	$50 \leq \tau_{0.55}\% < 66$ $\tau_{0.47}\% < 50$ or $\tau_{0.67}\% < 50$	$50 \leq \tau_F\% < 66$ $R < 0.4$
Red	$\tau_{0.55}\% < 50$ $\tau_{0.87}\% < 50$	$\tau_{0.55}\% < 50$ $\tau_{0.47}\% < 50$ or $\tau_{0.67}\% < 50$	$\tau_F\% < 50$ $R < 0.4$
Orange	$\tau_{0.55}\% < 50$ $\tau_{0.87}\% \geq 50$	$\tau_{0.55}\% < 50$ $\tau_{0.47}\% \geq 50$ and $\tau_{0.67}\% \geq 50$	$\tau_F\% < 50$ $R \geq 0.4$
Yellow	$50 \leq \tau_{0.55}\% < 66$ $50 \leq \tau_{0.87}\% < 66$	$50 \leq \tau_{0.55}\% < 66$ $\tau_{0.47}\% \geq 50$ and $\tau_{0.67}\% \geq 50$	$50 \leq \tau_F\% < 66$ $0.4 \leq R < 0.8$
Lime	$50 \leq \tau_{0.55}\% < 66$ $\tau_{0.87}\% \geq 66$	$50 \leq \tau_{0.55}\% < 66$ $\tau_{0.47}\% \geq 66$ or $\tau_{0.67}\% \geq 66$	$50 \leq \tau_F\% < 66$ $R \geq 0.8$

455 1: A) % of $\tau_{0.55}$ matches within EU, B) % of $\tau_{0.87}$ matches within EU; EU = $\pm(0.04+0.05\tau)$
456 2: A) % of $\tau_{0.55}$ matches within EU, B) % of $\tau_{0.47}$ matches within EU and/or % of $\tau_{0.67}$ matches within EU; EU =
457 $\pm(0.05+0.15\tau)$
458 3: A) % of τ_{ϕ} matches within EU, B) Correlation of τ_F ; EU = $\pm(0.05+0.05\tau)$
459 4: A) % of τ_{ϕ} matches within EU, B) Correlation of τ_F ; EU = $\pm(0.05+0.20\tau)$

460
461 Fig. 3 shows quality of site-by-site comparison of total and spectral AOD over land
462 during the summer from *Terra*, according to the color wheel of Fig. 2. To be included in
463 this figure, a site has at least 10 matches during a given season across all years. The
464 background image is a global surface reflectance (red, green and blue visible channels)
465 browse image pulled from the MODIS land team website
466 (<http://landweb.nascom.nasa.gov/cgi-bin/browse/browse.cgi>). Highlighted in Fig. 3 are
467 scatterplots at four sites (GSFC, Alta Floresta, Dalanzadgad, and Jabiru), demonstrating
468 why the site received a certain color symbol. AOD at GSFC (Maryland) is marked by
469 green because >66% match within EU in all three channels, whereas Alta Floresta
470 (Brazil) is marked by yellow because >50% but less than 66% match in all channels. At
471 Dalanzadgad (Mongolia), AOD at all channels compare poorly, and is given a red
472 symbol. Finally, Jabiru is given a blue symbol, because while AOD at 0.55 μm compares

473 favorably within EU, at 0.47 μm it does not. Also, at Dalanzadgad, MODIS tends to
474 overestimate AOD in clean conditions, whereas at Jabiru, MODIS tends to underestimate
475 in clean conditions, deriving negative values of AOD.

476

477 Fig. 4 shows the quality of the site-by-site comparison by season (Winter, Spring,
478 Summer, Fall), for *Terra*, superimposed on the global surface browse image (same as
479 used for Fig. 3). To be included on a panel, a site should have at least 10 matches during
480 a given season across all years. Because of seasonal changes in the surface or cloudiness,
481 or the ephemeral nature of certain AERONET sites, not all sites are represented for all
482 seasons. Although we plot results from Terra only, the maps (and discussions) are valid
483 for both instruments.

484

485 By looking at the collection of panels, one can visually assess where the MODIS retrieval
486 is performing well and also where it is not. Specific sites will be designated here (in the
487 text) by the names given by the AERONET web site (<http://aeronet.gsfc.nasa.gov>).

488 Much of the U.S. East Coast is plotted with green symbols over most seasons from both
489 instruments, signifying very good agreement. An exception is over New York City (the
490 CCNY and GISS sites, both near (40N, 73W)), where presumably, the urban surface is
491 poorly represented by MODIS's surface reflectance parameterization. Many sites in
492 Western Europe also compare well in all seasons, except for Venice (45N, 12E), a highly
493 urbanized coastal site with inland water. Essentially, the MODIS C005 was developed
494 based on the density of MODIS/AERONET collocations and AERONET sky retrievals
495 available through 2005. The U.S. East Coast and Western Europe were already well

496 sampled by AERONET, so that a robust characterization of both the aerosol (weakly
497 absorbing; *Levy et al.*, [2007b]) and surface properties (generally vegetated; *Levy et al.*,
498 [2007a]) were derived there. Therefore, it is not surprising that C005 products compare
499 well in these regions. It is also not surprising that the sites with consistently poor
500 comparisons are either heavily urbanized (CCNY, GISS and Venice) or have unique
501 surface characteristics (Palencia, in Spain, is on a plateau, and characterized by relatively
502 brighter surface, where the aerosol signal is comparatively weak for a dark-target
503 retrieval. Other regions that are generally well retrieved by MODIS include southern
504 Africa (e.g. Mongu (15S, 23E)), and the dark dense forests of the Amazon. These regions
505 were also marked by relatively dense AERONET sampling (prior to C005) and relatively
506 darker surfaces. We realize that the MODIS algorithm was well tuned for these regions.
507 There, however, are locations where the results compare well, even where there were few
508 or no AERONET measurements prior to C005. For example, sites over Japan and Korea
509 compare 66% within expected uncertainty. *Mi et al.*, [2007] demonstrated good
510 agreement for the Chinese sites of Taihu (31N, 120E) and Xianghe (39N, 116E). *Jethva*
511 *et al.*, [2007] found similar agreement over Kanpur (26N, 80E), India, which while the
512 general region is relatively bright, the immediate ~1km area around the sunphotometer is
513 anomalously densely vegetated.

514

515 Although showing where the MODIS algorithm is performing well is useful, Figs. 3 and
516 4 are also designed to discover regions and sites where the MODIS products do not
517 compare so well. In addition to some of the urban surfaces mentioned above, MODIS
518 compares poorly over brighter and elevated targets. These areas include the western U.S.,

519 (e.g. BSRN-Boulder (40N, 105W) and Sevilleta (34N, 106W)) the Patagonian region of
520 Argentina (e.g. Trelew (43S, 65W)), and the steppe and near desert plateaus of Russia
521 and China (e.g. Irkutsk (51N, 103E) and Dalanzadgad). These scenes are too bright for
522 optimal dark target algorithm performance, but do not exceed a brightness threshold test
523 that would result in lowered QC (scene reflectance > 0.25 at $2.1 \mu\text{m}$; [Levy *et al.*,
524 2007b]). These regions may be better suited for retrieval with the Deep Blue algorithm
525 [Hsu *et al.*, 2004]. Some of these regions are also marked by aerosol type that would not
526 have been characterized by the clustering of AERONET data available in 2005.

527

528 We also find regions where we had expected better comparison - because the particular
529 AERONET sites were available during the processing of C004, and thus used for
530 developing C005. For example, Alta_Floresta (9S, 56W) and CUIABA-MIRANDA
531 (15S, 56W) are located in Brazil, one near the border of the Amazon forest, the other
532 located further south in the cerrado (savanna-like vegetation). Alta_Floresta is marked by
533 green in some seasons (winter and fall), and yellow or red in the others. Cuiaba is
534 generally marked red in all seasons. The scatter plots associated with these sites suggest
535 that AOD is generally overestimated, especially as the loading increases. This is
536 consistent with a scenario in which the assumed aerosol type has too much absorption in
537 the optical model [e.g. Ichoku *et al.*, 2003]. In other words, in this region the *single*
538 *scattering albedo*, or *SSA* is assumed too low. During the development of the C005
539 aerosol models, Levy *et al.*, [2007b] found that the aerosol type in the region would
540 sometimes tend toward more absorbing particles ($\text{SSA} \sim 0.86$ at $0.55 \mu\text{m}$), or toward more
541 moderate absorption ($\text{SSA} \sim 0.91$), with a tendency to be more absorbing towards the

542 southeast. Boxes were drawn on a map to signify where and when the stronger absorbing
543 type should be preferred, and these borders were somewhat arbitrary. We believe that the
544 box designating absorbing aerosol type was drawn too far west, which caused some of
545 the systematic bias in high AOD conditions over Cuiaba. For example, AERONET
546 Version 2 sun retrievals (<http://aeronet.gsfc.nasa.gov>) suggest that SSA over Cuiaba is
547 closer to 0.9 during the dry season. Even the C005 moderately absorbing aerosol type
548 may be too strong for characterizing Alta_Floresta, where SSA~0.91-0.92 would be more
549 appropriate [Schafer et al. (2008; JGR)].

550

551 The last site we will explore here is Jabiru (12S, 132E) in northern Australia. This site
552 has generally low AOD, and MODIS tends to derive negative AOD in these conditions
553 [Remer et al., 2008]. This is a systematic bias that results from overestimating surface
554 reflectance in the visible channels. One possible reason is the presence of red soil, which
555 may not display the same surface reflectance relationships as modeled with the C005
556 parameterization. Other regions, such as Brazil (including Alta_Floresta) during the
557 rainy season, also show MODIS underestimation in clean conditions that may be a result
558 of some other surface issue. Exploring and correcting for this negative bias is a subject
559 of future study.

560

561 **3.2 Total AOD over ocean**

562

563 Fig. 5 displays the results of our collocation (including filtering for $QC \geq 1$ and
564 AERONET site elevations less than 250 m above sea level), for total AOD (at 0.55 μm)

565 over ocean, for Terra (left) and Aqua (right). Like Fig. 1, the color for each ordered pair
566 represents the number of such matchups. The dashed, dotted and solid lines are the 1-1
567 line, EU for ocean AOD ($\tau_{EU} = \pm(0.03+0.05\tau)$), and the linear regression of the pre-sorted
568 scatterplot, respectively. Also given for each plot are number of collocations (N), the
569 percent within EU, the regression curve, correlation (R), and the RMS error of the fit.
570 The plots show the quality of the matching, as both Terra and Aqua regressions hug the
571 1-1 line through the majority of the data, have slopes near 1, y-intercepts near zero, and
572 $R > 0.9$. One can see the relative dominance of $AOD < 0.15$, with decreasing numbers of
573 points towards the axes limits. There is little statistical difference between the overall fits
574 of Terra and Aqua, although Aqua's slope is further from 1.0 (0.91) than Terra's (0.97).
575 For both instruments, less than 59% of the points lie within the dotted lines representing
576 EU. Table 2 provides some statistics of the comparison for $0.55 \mu\text{m}$, as well as the
577 comparison at $0.86 \mu\text{m}$. At $0.86 \mu\text{m}$, the percent within EU is slightly better, but still not
578 at the required 66% level required for validation. By slightly relaxing our EU bars to
579 $\pm(0.04+0.05\tau)$, we can get to the >66% level (last column in Table 2). Nearly 75% fall
580 within the interval $\pm(0.05+0.05\tau)$ originally defined by *Tanré et al.*, [1997]. In keeping
581 with our requirement of 66%, we claim over-ocean EU for C005 AOD to be

$$582 \quad \tau_{EU} = \pm(0.04+0.05\tau). \quad (4)$$

583 We denote this revised EU interval by the term “new” (as compared to the “old” defined
584 by Remer et al., 2005 for C004). In some sense, since >66% of C004 dataset fell within
585 the old EU, C005 seems not as good as C004. We note, however, that some of the
586 difference is due to slight changes in MODIS calibration of C005 radiances [e.g.,
587 Redemann et al., 2009].

588

589 **Table 3: Statistics of the comparison between MODIS (Terra and Aqua) and**
590 **AERONET total spectral AOD over ocean. The number of points (N) is 13,773**
591 **(10,407) for Terra (Aqua). The last two columns represent the % within EU at the**
592 **old and new intervals.**

Sat	Wave (μm)	Mean AOD AERO	Mean AOD MODIS	Regression equation	R	RMS	% in old	% in new
Terra	0.87	0.166	0.183	y = 0.976x + 0.015	0.913	0.077	59.99	69.74
Terra	0.55	0.192	0.210	y = 0.976x + 0.018	0.912	0.083	57.03	66.20
Aqua	0.87	0.174	0.177	y = 0.903x + 0.015	0.916	0.070	62.43	72.04
Aqua	0.55	0.201	0.205	y = 0.910x + 0.017	0.911	0.078	58.59	68.01

593 old: $\tau_{EU} = \pm(0.03+0.05\tau)$; new: $\tau_{EU} = \pm(0.04+0.05\tau)$

594

595 Table 3 points out an interesting difference between Terra and Aqua. Although the
596 regression slopes for Terra are close to 1.0 in both wavelengths, the mean AOD for
597 MODIS is 0.02 higher than for AERONET. The Aqua mean AOD is much closer to
598 AERONET. To examine this issue, we perform another regression, this time excluding
599 the extreme AOD events (7%) where AOD > 0.5 (according to AERONET). The results
600 are presented in Table 4. Without the extreme events, Terra’s mean bias, is still 0.017,
601 which is more than 10% error. This discrepancy is consistent with that found by *Remer*
602 *et al.*, [2008] as a difference between Terra and Aqua time series. We believe that this is
603 bias of Terra (but not of Aqua).

604

605 **Table 4: Statistics of the comparison between MODIS (Terra and Aqua) and**
606 **AERONET total spectral AOD over ocean, limited to AERONET AOD < 0.5. The**
607 **number of points (N) is 12,914 (9704) for Terra (Aqua). The last column is the %**
608 **within EU (new) interval.**

Sat	Wave (μm)	Mean AOD AERO	Mean AOD MODIS	Regression equation	R	RMS	% in new
Terra	0.87	0.134	0.151	y = 0.973x + 0.015	0.859	0.060	71.76
Terra	0.55	0.157	0.175	y = 0.972x + 0.018	0.867	0.064	68.11
Aqua	0.87	0.140	0.146	y = 0.901x + 0.015	0.885	0.050	74.64

Aqua	0.55	0.164	0.171	$y = 0.901x + 0.018$	0.884	0.056	70.52
------	------	-------	-------	----------------------	-------	-------	-------

609 New EU: $\tau_{EU} = \pm(0.04+0.05\tau)$

610

611 As we performed for over-land validation, we can create scatterplots to study the quality
612 of the MODIS/AERONET comparison site-by-site over ocean. We summarize the results
613 of the scatterplots on a global map, using the color wheel shown in Fig. 2, and the column
614 from Table 2 for ‘AOD ocean’. Since the comparison is for two wavelengths (0.55 and
615 0.86 μm) rather than three, the conditions for each color are different than for over land.
616 A “good” site (green) is one where MODIS/AERONET AOD in both channels show
617 66% match within the new EU bars. A “bad” site (red) is where both channels show
618 <50% match. Circling from green to red counterclockwise (colder colors) represents sites
619 where the 0.55 μm channel compares favorably, but 0.86 μm compares increasingly
620 poorly. Clockwise (warmer colors) represents sites that have poor comparison at 0.55
621 μm , but better comparison at 0.86 μm .

622

623 Like Fig. 3 over land, Fig. 6 displays the quality of MODIS (Terra) versus AERONET
624 comparison for the sites used for evaluating over-ocean pixels during the summer. Also
625 displayed are scatterplots from four sites, as examples of the different matchup
626 characteristics (colors). It is interesting that while the collection of all comparisons looks
627 extremely good in the global scatterplot (Fig. 5) the site-by-site comparisons do not look
628 as consistently good. Fig. 7 displays comparisons of MODIS-Terra and AERONET for
629 all seasons. Although, there is some difference between the distribution of colors
630 between the Terra and Aqua maps, in general they are consistent, so only Terra is plotted
631 here. Coastal sites along the U.S. East Coast (e.g., COVE (36N, 75W)) and Western

632 Europe (e.g. Venice (45N, 12E)) compare very well in both channels, during the winter
633 and fall seasons. Over these regions, the comparison is worse in the spring and summer,
634 especially for the 0.86 μm (blue and purple colors). During the summer, AOD derived
635 over Saharan and Asian dust belts (e.g., Capo_Verde (16N, 22W), La_Parguera (17N,
636 67W), Shirahama (33N, 135E)), has errors at 0.55 μm , but most significantly at 0.86 μm
637 (red and purple). This behavior is consistent with the sort of dust non-sphericity induced
638 error suggested by *Levy et al.*, [2003]. MODIS retrievals near remote ocean island sites
639 (e.g. Lanai (20N, 156W), Tahiti (17S, 149W), Guam (13N, 144E)) seem reasonable,
640 although there are relatively few collocations, due to the temporary nature of these sites
641 coupled with persistent cloudiness. Due to lack of financial support, the Lanai site was
642 abandoned after 2003, and the Tahiti site has maintenance issues.

643

644 Ascension_Island (7S, 14W) provides long-term collocation, but has varied quality of
645 spectral AOD comparison over both instruments and all seasons. All individual
646 scatterplots, however, (not plotted) indicate significant y-offset (>0.1) and slope less than
647 one (<0.8) at all wavelengths. Ascension_Island is an interesting site, because it is
648 remote, yet is influenced by long-range transport of a variety of aerosol types during
649 different seasons, such as Saharan dust and West African biomass-burning smoke in
650 Winter, and Brazilian and southern African smoke in Summer.

651

652 **4.0 Comparison of aerosol size parameters**

653

654 Good or bad, we desire to characterize the EU for the aerosol size information (i.e. α and
655 fAOD) over both land and ocean. We apply the same MODIS/AERONET matching
656 strategy as for the total AOD, filtering by the number of valid pixels for MODIS (≥ 5 out
657 of 25) and valid measurements per hour (≥ 2) for AERONET. We filter by QC threshold
658 (QC=3 for land and QC ≥ 1 for ocean). We filter for scenes with low variability of
659 elevation. We note, however, that according to the QA plan, the operational retrieval will
660 not report valid size parameters for all retrieved pixels. For example, over land, the
661 retrieval reports Ångström exponent only when the retrieved total AOD is positive ($\tau > 0$).
662 Reporting FF requires even larger aerosol signal ($\tau > 0.2$ at $0.55 \mu\text{m}$). The fAOD,
663 however, is reported for all retrieved values of AOD (if AOD is negative, fAOD is given
664 the value of zero). Over ocean, although there is no operational filtering of size products
665 based on retrieved total AOD or QA results, we choose to further filter during our
666 collocation process, thus ensuring sufficient aerosol signal.

667

668 **4.1 Ångström Exponent and fAOD over land**

669

670 The fundamental retrieved products of the C005 over-land algorithm are the total AOD at
671 $0.55 \mu\text{m}$, the fine mode fraction (FF), and the surface reflectance at $2.1 \mu\text{m}$. The FF is
672 incremented by 0.1 (from -0.1 to 1.1), and the other two parameters are fitted to the
673 observed spectral reflectance, given the constraints of VIS/SWIR surface reflectance
674 parameterization and seasonally/regionally defined fine dominated aerosol type. Note,
675 that in the case of non-physical FF retrieval (-0.1 or 1.1), the FF would be adjusted to 0.0
676 or 1.0, and other parameters adjusted accordingly. Based on the C005 development test-

677 bed [Levy *et al.*, 2007b], about 10% of cases resulted in non-physical FF. From
 678 sensitivity tests [Levy *et al.*, 2007b], we expected robust retrieval of total AOD, which
 679 was confirmed in section 3.1. Although the sensitivity tests and preliminary validation
 680 did not suggest significant improvement for C005 size parameters, we use this
 681 opportunity to characterize the products.

682

683 The Ångström exponent over land (α_L), derived by MODIS, relates the AOD at 0.47 and
 684 0.66 μm (Eq 1). Since AERONET-derived AOD can be interpolated to MODIS
 685 wavelengths by quadratic interpolation [Eck *et al.*, 1999], a comparable AERONET α_L
 686 can easily be derived. Although the operational algorithm requires only positive AOD,
 687 we shall require here that $\tau > 0.2$. Thus, there are 11,184 (7019) collocations for Terra
 688 (Aqua) over land, which are plotted as density scatterplots in Fig. 8, with statistics
 689 described in Table 5.

690 **Table 5 Statistics of the comparison between MODIS (Terra and Aqua) and**
 691 **AERONET Ångström exponent over land. The number of points (N) is 11,184**
 692 **(7019) for Terra (Aqua).**

Sat	Mean α_L AERO	Mean α_L MODIS	Regression Eq	R	rms of fit	% within ± 0.45
Terra	1.295	1.145	$y = 0.656x + 0.334$	0.554	0.390	68.95
Aqua	1.265	1.125	$y = 0.629x + 0.339$	0.555	0.380	68.94

693

694 Although the mean values of Ångström exponent provided by either MODIS are both
 695 similar to AERONET ($\alpha_L \sim 1.2$), it is clear that MODIS has little skill at deriving it. The
 696 dynamic range derived from MODIS ($0.5 < \alpha_L < 1.8$), limited by the choice of MODIS
 697 aerosol models, is smaller than that derived by AERONET (generally $0.0 < \alpha_L < 2.2$). The
 698 correlations for α_L are much lower ($R \sim 0.55$) than for the total AOD or even the spectral

699 AOD. In addition, the slopes are much less than one (~ 0.63) and the y-offsets are much
700 larger than zero (~ 0.33). Yet we can assign EU for Ångström exponent over land ($\alpha_{L,EU}$),

$$701 \quad \alpha_{L,EU} = \pm 0.45 \quad (6)$$

702 so that 66% of the MODIS/AERONET matches are contained within them. These are
703 placed on Fig 8 as the dashed lines. Of course, our eyes are drawn to the many points at
704 the boundaries of MODIS retrieval space (e.g. $\alpha_L \sim 0.6$ for dust model or ~ 1.8 for fine-
705 dominated models) regardless of what is derived by AERONET. Other than the
706 extremely dense line of points where MODIS retrieves $\alpha_L \sim 0.6$, the blue colors suggest
707 that MODIS and AERONET agree for some scenes with fine-dominated aerosols
708 ($\alpha_L > 1.5$). There are many points, however, where alpha ~ 1.2 - 1.7 from AERONET
709 paired with 0.6 - 1.2 for MODIS.

710

711 Note that due to the small separation between the two wavelengths (0.47 and $0.66 \mu\text{m}$),
712 measurement uncertainties in either channel can lead to large errors in deriving α . For
713 example, we can envision a scene with modest signal (say $\tau = 0.28, 0.20$ and 0.16 at $0.47,$
714 0.55 and $0.66 \mu\text{m}$, respectively). Even if spectral AOD can be measured within ± 0.01
715 (e.g. by AERONET), the “true” $0.47/0.66$ Ångström exponent value ($\alpha_L = 1.58$) could be
716 reported within ± 0.28 (between 1.30 and 1.85). Therefore, while MODIS/AERONET
717 matching is poor (± 0.45), it is not unexpectedly poor. Further restricting AOD to ($\tau > 0.4$)
718 leads to better correlation ($R = 0.68$) and smaller EU (± 0.4), but still, we cannot claim the
719 over-land Ångström exponent to be a quantitative measure.

720

721 Although MODIS estimates of Angstrom exponent are clearly not useful globally, we can
 722 try to identify where it has some value. We again look at individual scatterplots, for
 723 specific sites and season. Fig. 9 shows MODIS versus AERONET derived Ångström
 724 exponent at GSFC (39N, 77W) during the summertime. Here, there is qualitative success
 725 of retrieving the appropriate dynamic range covered by AERONET. Although the slope
 726 is not one to one, the correlation is reasonable ($R=0.71$), 73% fit within ± 0.45 , and 66%
 727 fit within ± 0.3 .

728 The Ångström exponent is poorly derived because it is limited to the set of C005 aerosol
 729 models, which are in turn limited in dynamic range. We might consider whether there is
 730 instead a better constraint on fAOD. From AERONET, we compute fAOD from the
 731 sun-measured spectral AOD, following version 4 of the spectral deconvolution algorithm
 732 [O'Neill *et al.*, 2003] and assuming the 'Continental' aerosol model. The fAOD is
 733 defined regardless of total AOD, so we do not need to constrain to $\tau > 0.2$ to have low
 734 uncertainty in its magnitude. Thus we can assess the full number of collocations (37,553
 735 and 22,773 for Terra and Aqua). The scatterplot is presented as Fig. 10, with statistics
 736 listed in Table 6.

737 **Table 6 Statistics of the comparison between MODIS (Terra and Aqua) and**
 738 **AERONET derived fAOD over land. The number of points (N) is 37,553 (22,773)**
 739 **for Terra (Aqua).**

Sat	Mean fAOD AERO	Mean fAOD MODIS	Regression Eq	R	rms of fit	% within $\pm(0.05+0.20\tau)$
Terra	0.151	0.090	$y = 0.644x + -0.013$	0.817	0.120	66.15
Aqua	0.144	0.082	$y = 0.577x + -0.010$	0.787	0.118	66.62

740

741

742 The fAOD scatterplot (Fig. 10) shows many points near the one-to-one line. However,
743 there are also a significant number of cases where MODIS is retrieving fAOD = 0.0
744 (approximately 10%), resulting in large differences between mean values (~0.08 for
745 MODIS, ~0.151 for AERONET). Nonetheless, by setting EU bars for the fAOD over
746 land as

$$747 \quad \tau_{f,EU} = \pm(0.05+0.20\tau) \quad (7)$$

748 we can contain that 66% of the matched pairs, globally

749

750 Like we did for total AOD, we use the color wheel of Fig. 2 and Table 2, to assess the
751 quality of the seasonal site by site comparisons. Instead of test B being based on EU for
752 a different wavelength, the test B considers the magnitude of the correlation at the given
753 site. In other words, “good” means correlation ($R > 0.8$) whereas “bad” means
754 correlation ($R < 0.4$). The joint results of both tests A and B determine the color of the
755 symbol designated at the site. For Terra, the results for each site, for each season are
756 displayed by Fig. 11.

757

758 Overall, the best overall matches are for the eastern half of the U.S. during the summer.
759 Both the correlation and number of matches within EU are high. This is not surprising
760 given the plethora of AERONET information obtained for this region during C005
761 development. The worst performance (red colors) is seen at the semi-bright sites that
762 surround the deserts of the world. Of course this is also expected.

763

764 We can only begin to assess the quality of the fAOD at the other sites. The U.S. East
765 Coast during the winter and spring consistently shows cyan or blue colors, indicating
766 good matching within EU, but with low correlation. This may indicate that, although the
767 MODIS assumptions are generally correct for these regions/seasons with low signal,
768 there is low sensitivity to small perturbations.

769

770 Given the dominance of green and bluish colors throughout the globe, we believe that the
771 “true” conditions are generally well captured by the C005 LUT and surface
772 parameterizations. Still, however, the MODIS estimates of fAOD are clearly wrong in
773 some areas, even when there should be sufficient aerosol signal. For example, although
774 AOD from MODIS compares well to AERONET at Kanpur, India, *Jethva et al.*, [2007]
775 pointed out that C005 will almost exclusively retrieve dust (coarse-dominated aerosol),
776 during the fall and winter, when pollution (fine aerosol) should have been dominant.

777 Similar behavior is demonstrated in Fig 11, as indicated by the purple and red symbols.

778 We performed a sensitivity study that suggested that if the assumed seasonal aerosol type
779 was highly absorbing (SSA~0.86) instead of the (default) moderately absorbing model
780 (SSA~0.91), the number of false dust retrievals would be reduced. A slight revision of
781 surface reflectance parameterization would also help. Evaluation of revised AERONET
782 data (known as Version 2; <http://aeronet.gsfc.nasa.gov>) confirms that the aerosol at
783 Kanpur during the fall and winter may be more absorbing (~0.87-0.88) than previously
784 believed.

785

786 For sites, such Kanpur, the aerosol signal is so strong there that better constrained surface
 787 and aerosol models will help. Over the bulk of the globe, however, the MODIS
 788 observations are likely to be insufficient for retrieving aerosol size parameters over land,
 789 meaning that external and/or additional constraint information (say from a model or
 790 another satellite product) may be required.

791

792 **4.2 Ångström Exponent and fAOD over ocean**

793

794 Although MODIS was not expected to, and does not, derive accurate aerosol size
 795 properties over all land surfaces, it was expected that it would do better over ocean. Fig.
 796 12 and Table 7 compare the over water Ångström exponent (α_o), defined using 0.55 and
 797 0.86 μm , constrained where total AOD > 0.15. Although this constraint is inconsistent
 798 with over land (AOD > 0.2), we use it because we expect better sensitivity over ocean,
 799 and it is consistent with a constraint used by Remer et al., [2005]. Fig. 13 and Table 8
 800 assess derived fAOD for all collocations (not filtered by AOD).

801

802 **Table 7 Statistics of the comparison between MODIS (Terra and Aqua) and**
 803 **AERONET Ångström exponent over ocean ($\tau > 0.15$). The number of points (N) is**
 804 **4259 (3287) for Terra (Aqua).**

Sat	Mean α_o AERO	Mean α_o MODIS	Regression Eq	R	rms of fit	% within ± 0.3
Terra	0.943	0.867	$y = 0.685x + 0.211$	0.873	0.227	69.88
Aqua	0.880	0.864	$y = 0.630x + 0.311$	0.833	0.233	64.47

805

806 **Table 8 Statistics of the comparison between MODIS (Terra and Aqua) and**
 807 **AERONET fAOD over ocean. The number of points (N) is 13,773 (10,407) for**
 808 **Terra (Aqua).**

Sat	Mean fAOD AERO	Mean fAOD MODIS	Regression Eq	R	rms of fit	% within $\pm(0.04+0.05\tau_f)$
Terra	0.118	0.125	$y = 0.809x + 0.023$	0.846	0.059	67.12
Aqua	0.120	0.122	$y = 0.718x + 0.028$	0.799	0.061	64.79

809

810 Over ocean, the mean values of Ångström exponent derived by MODIS and AERONET
811 are similar ($\alpha_0 \sim 0.9$), and both MODIS instruments show skill at deriving it. Over ocean,
812 the dynamic range derived from MODIS ($-0.2 < \alpha_0 < 3.0$) seems sufficient at capturing the
813 range of AERONET. Although the correlations for α_0 are not much lower ($R = 0.873$
814 and 0.833 for Terra and Aqua, respectively) than for the total AOD, their slopes are much
815 less than one ($=0.685$ and 0.630) with y-offsets much larger than zero ($=0.21$ and 0.31).
816 Whereas both instruments showed nearly identical regressions over land, there are
817 differences to the MODIS/AERONET Ångström exponent comparisons between Terra
818 and Aqua. It is interesting that although the AERONET mean during Aqua overpass is
819 lower ($\alpha_0 = 0.88$ than that for Terra ($\alpha_0 = 0.94$), both MODIS instruments derive
820 $\alpha_0 \sim 0.865$. The difference in AERONET means may be in part due to different sites
821 representing different years for Terra and Aqua, which is not equally captured by the two
822 satellites. While both satellite instruments underestimate their respective means, Terra's
823 bias is even more pronounced. However, the regression coefficients for Terra are
824 generally better than those for Aqua. Here, we assign EU of ocean Ångström exponent
825 as

$$826 \quad \alpha_{0,EU} = \pm 0.3, \quad (8)$$

827 so that approximately 66% of the MODIS/AERONET matches are contained within
828 them. These are placed on Fig. 12 as the dashed lines.

829

830 The mean values of the fAOD (~ 0.12) are very similar for MODIS and AERONET, as
831 well as similar for both MODIS overpasses. However, we note that both regressions
832 show less than one slope (< 0.81) and positive y-offsets (> 0.02). Like shown for α_o , the
833 mean fAOD seems to match somewhat less for Terra than Aqua, although the regression
834 coefficients are stronger. We set EU for fAOD (τ_{fEU}) over ocean as

$$835 \quad \tau_{fEU} = \pm(0.04 + 0.05\tau_f). \quad (9)$$

836 to contain approximately 66% of the points of Fig. 13 (dashed lines). Most of the
837 collocations are clustered at low AOD (measured by AERONET), however there are a
838 few points at higher fAOD. These high fAOD points are generally underestimated by
839 MODIS. We realize, although we successfully defined EU for fAOD over ocean, that it
840 does not fully characterize the distribution of the biases displayed by Fig 13.

841

842 Essentially, we believe the discrepancies between MODIS and AERONET over ocean
843 are mainly a result of discrepancies in assumed versus real aerosol optical properties.
844 Because of retrieval artifacts seen in dust environments (because of dust non-sphericity),
845 MODIS will compensate by using larger amounts of fine mode to fit the spectral
846 reflectance. Thus, it tends to overestimate Ångström exponent and underestimate aerosol
847 size in dusty conditions. The fAOD may be overestimated. Because the C005 aerosol
848 models [Remer *et al.*, 2006] over ocean do not include much absorption, cases of
849 pollution with significant black carbon content and certain biomass burning cannot be
850 correctly fitted to the spectral reflectance. The MODIS algorithm will compensate by
851 using a larger particle, and thus underestimate Ångström exponent and overestimate
852 aerosol size. The fAOD will be underestimated in these conditions.

853

854 Once more, we describe a color wheel (Fig. 2 plus Table 2) to indicate, site-by-site and
855 seasonally, the quality of fAOD comparison with AERONET. We represent the quality of
856 comparison, in both expected uncertainty and correlation space. We set a “good”
857 comparison (green) where >66% of collocations fall with expected uncertainty
858 ($\pm(0.05+0.05\tau)$) and have correlation coefficients ($R>0.8$). A “bad” comparison (red)
859 describes a comparison where <50% fall within uncertainty bars, and have $R<0.4$. Going
860 counterclockwise (cooler colors) are cases with higher %, but lower correlation, whereas
861 going clockwise (warmer colors) represents the opposite. The results are presented as
862 Fig. 14.

863

864 Generally, Fig. 14 shows that in much of the globe, fAOD compares within EU (green,
865 cyan and blue colors). However, at most sites, the correlation is lower than the global
866 value of 0.8. Most of these points indicate that neither dust nor biomass burning are
867 dominant. The worst overall comparisons are seen at sites in the path of Asian aerosol
868 transport (expected mix of pollution and dust), especially during the spring maximums.
869 The correlation is almost always low ($R<0.4$) in the paths of Atlantic and Pacific dust,
870 and higher in Europe. Although we do not display the plot for Aqua, we note that the
871 symbols have similar color distributions. An interesting exception is over the dust belts,
872 where there are more blue symbols, suggesting more matches within EU, but still with
873 low correlation.

874

875 **5.0 Changes of AOD comparison over time**

876

877 If we desire to use the MODIS data record for assessment of aerosol trend, we must
878 demonstrate that there is no trend inherent in the MODIS instruments. We have already
879 seen that there is a ~ 0.015 offset between Terra and Aqua over ocean (*Remer et al.*,
880 [2008]) with no such offset over land. This, we understand is a result of absolute
881 calibration differences (of less than the required 2%) in one or more channels used for the
882 over ocean retrieval, that may not be used for retrieving over land. To believe in any
883 MODIS derived aerosol trend, we must also demonstrate that the MODIS aerosol
884 products are not changing in time.

885

886 We know that the MODIS calibrations are continuously being updated due to systematic
887 degradation in sensor optics and electronics (e.g. Xiong et al., 2008). We would like to
888 know whether these continuous updates have successfully maintained the accuracy of the
889 MODIS observed spectral reflectances over time. We, however, do not have a known
890 “truth” for assessing observed (top of atmosphere) spectral radiance, everywhere and
891 throughout time. For successful retrieval of ocean color products, the MODIS ocean color
892 team (<http://oceancolor.gsfc.nasa.gov>) requires better than 2% accuracy for measured
893 radiance in low light. To attain that accuracy, they continuously perform *vicarious*
894 calibration, meaning that they adjust the MODIS calibration coefficients so that a
895 retrieved product will match a ground truth measurement of a particular ocean color
896 parameter [*Franz et al.*, 2007]. This sort of tuning keeps the MODIS record consistent
897 with surface measurements and measurements of previous ocean color measurement
898 missions. However, 1) the vicarious calibration is over one site only, 2) it is intended for

899 very low light conditions over the ocean (far from glint, clouds, land, and thick aerosol),
 900 and 3) the ocean color channels do not include the NIR and SWIR channels used for the
 901 dark target aerosol retrieval. The aerosol retrieval is not limited to the conditions at one
 902 site, and must work over medium and brighter surfaces over land and in heavy aerosol
 903 loadings.

904
 905 We have the advantage of being able to evaluate the MODIS aerosol retrieval at multiple
 906 AERONET sites, including some that have operated throughout a long duration of the
 907 MODIS observing period. Table 9 lists selected AERONET sites with a seven-year or
 908 longer record, identifying which are used to evaluate over land and/or ocean aerosol
 909 retrievals.

910 **Table 9: AERONET sites with long-term records used for time series assessment**

Site Name	(Lat, Long)	Land and/or Ocean
Alta Floresta	(9S,56W)	L
Ascension Island	(7S,14W)	O
Banizoumbou	(13N,2E)	L
BONDVILLE	(40N,88W)	L
Capo Verde	(16N,22W)	O
Cart Site	(36N,97W)	L
Dakar	(14N,16W)	L, O
Dalanzadgad	(43N,104E)	L
El Arenosillo	(37N,6W)	L, O
GSFC	(38N,76W)	L
Ispra	(45N,8E)	L
Mongu	(15S,23E)	L
Ouagadougou	(12N,1W)	L
Sevilleta	(34N,106W)	L
Skukuza	(24S,31E)	L
Venise	(45N,12E)	L, O

911
 912 Like *Mi et al* [2007], we define the *Fraction of Expected Uncertainty (FEU)* for AOD as

913
$$FEU = \frac{\tau_{MODIS} - \tau_{AERONET}}{|\tau_{EU}|}, \quad (10)$$

914 where the $||$ is the magnitude of the EU for the matched parameter (e.g. $(A+B\tau)$ as
915 defined in Eq. 2). Thus, $|FEU| \leq 1$ represents the case where MODIS agrees with
916 AERONET within EU (a “good” match), and $|FEU| > 1$ represents a case where it does not
917 (a “bad” match). In addition, the signed value of the FEU denotes whether MODIS is
918 biased high (positive) or low (negative) compared to AERONET.

919
920 We assume that the measurement errors from the collection of AERONET instruments
921 are random, so that we can plot the time series of the FEU. A change in FEU
922 (MODIS/AERONET comparison) over time would indicate that MODIS is changing
923 over time. Fig. 15 plots the time series of FEU for Terra (left) and Aqua (right) over land,
924 where the EU is defined by Eq. 3. We use all collocations from the over-land sites listed
925 in Table 9, providing 6512 for Terra and 3402 for Aqua.

926
927 For Aqua, (from 2002 through 2008), there is no clear or significant trend in the FEU.
928 Overall, there is a slight negative bias shown by MODIS, which is consistent to that
929 suggested by Table 1 (for all MODIS/AERONET collocations). For Terra, however,
930 there is a statistically significant trend, as measured by a T-test with 6512 points and
931 correlation of $R=0.215$. Early in the Terra mission, MODIS is biased high, which
932 becomes a low bias sometime after 2004 (near day 1500). Averaged over the entire time
933 series (as in Table 1 for all collocations), however, MODIS-Terra shows no bias.

934

935 Over ocean, we define the AOD EU by Eq. 4. We use all collocations for the over-ocean
936 sites listed in Table 9, providing 2055 points for Terra and 1767 for Aqua. Fig. 16 shows
937 that there is no significant trend for FEU for either Terra or Aqua over ocean. There is a
938 small positive bias to Terra with an even smaller negative bias to Aqua. Again, these
939 results are consistent with those of Table 3, for all collocations over ocean.

940

941 Based on Figs. 15 and 16, we do not have enough information to explain why only
942 Terra's over land retrieval is changing. Analysis of spectral AOD show that all channels
943 show a similar trend. Except for a few sites, most of the long-term AERONET stations
944 are characterized by discrete episodes of high AOD. Thus, when we try to filter by the
945 additional criteria of sufficient AOD signal (e.g. $\tau \geq 0.2$ over land or $\tau \geq 0.15$ over ocean),
946 the statistics of fAOD and Ångström exponent become rather sparse. Time series of size
947 parameter FEU are not as easy to interpret, and therefore are beyond the scope of this
948 paper.

949

950 However, we recall that the over land retrieval inverts reflectance in three channels (0.47,
951 0.66 and 2.1 μm), whereas the over ocean aerosol retrieval inverts in six channels (0.55,
952 0.66, 0.86, 1.24, 1.64 and 2.12 μm). The 0.47 μm channel is used for land and not for
953 ocean aerosol retrieval, and like other blue and deep blue channels (e.g. 0.412 and 0.443
954 μm) aboard MODIS, it is affected by polarization and directional signal issues. This is
955 especially true for Terra, which suffers from more significant optical sensor degradation
956 than does Aqua (X. Xiong, personal communication). However, unlike the 0.412 and
957 0.443 μm channels, which are closely monitored by the ocean color team

958 (http://oceancolor.gsfc.nasa.gov/VALIDATION/operational_gains.html) and tuned for
959 the bio-optical retrieval algorithms, the 0.47 μm channel may have residual calibration
960 error. Sensitivity tests show that it is entirely possible that a systematic change in the
961 0.47 μm channel is capable of driving the trend seen in MODIS-Terra's FEU record.
962 Preliminary analysis of the 0.47 μm reflectance, included with our MODIS/AERONET
963 collocations over ocean (which has no trend in AOD FEU), suggest that there is such a
964 residual time dependent trend. Although it is beyond the scope of this paper to analyze
965 for statistical significance and other details, we can see how the process of MODIS
966 validation can help reveal hidden biases or uncertainties in the calibration algorithms.

967

968 **6.0 Conclusions**

969

970 As a result of deficiencies observed for previous versions/collections of MODIS aerosol
971 products over ocean and dark-land targets [e.g., *Remer et al.*, 2005; *Levy et al.*, 2005], a
972 new version of the MODIS dark-target algorithm was developed [*Levy et al.*, 2007a;
973 2007b; *Remer et al.*, 2006], and used for deriving Collection 5 (C005). Here, we used
974 ground truth sunphotometer (AERONET) data to evaluate eight years of the MODIS
975 dark-target products, including the total AOD and several aerosol size products. We
976 defined an expected uncertainty (EU) for a given parameter, which is an envelope that
977 contains at least 66% of the matched pairs (MODIS versus AERONET). Some of the
978 products we consider to be *validated* within their expected EU, although it is up to data
979 users to decide whether our defined EU is small enough for a particular application.

980

981 Over dark-land targets, more than 69% of MODIS total AOD at several wavelengths
982 (nominally 0.55 μm) matched those of AERONET within the EU defined by previous
983 studies (i.e., $\tau_{EU} = \pm(0.05+0.15\tau)$). This satisfied our validation criteria. Over ocean, we
984 found that the EU defined by previous evaluations was too restrictive. However, by
985 slightly relaxing the EU to $\pm(0.04\pm 0.05\tau)$ satisfied the 66% matching requirement for
986 validation.

987

988 Although we demonstrated *global* validation of total AOD over each surface type, we
989 expected that there might be systematic discrepancies over certain regions and/or seasons.
990 We created a metric to assess the quality of the comparison, site by site, season by
991 season, and separated by land and ocean as well as by Terra and Aqua. We defined a
992 “good” comparison to be one where >66% of MODIS/AERONET pairs matched within
993 EU at a particular site and season, and a “bad” comparison to be one where <50% were
994 matched within EU. In general, over-land AOD was well matched in regions that were
995 both vegetated (dark targets optimal for the MODIS algorithm), and also extensively
996 sampled by AERONET prior to the development of the algorithm. These included the
997 eastern United States, Western Europe and Southern Africa. Some regions, like
998 southeastern Asia, were not previously sampled by AERONET, but compared well
999 because they have similar surface properties. Although expected for a dark-target
1000 algorithm, poor comparisons were seen over brighter and elevated targets, such as the
1001 western United States and central Asia. Discrepancies were also seen over northern
1002 Australia and other areas known for reddish color soils. Yet, despite prior AERONET
1003 sampling and generally dark enough surface, we found poor comparison over the

1004 Brazilian savanna that implied that the aerosol model assumed for MODIS had a single
1005 scattering albedo that was too low. Over ocean, the poorest comparisons were either in
1006 the known dust transport pathways (e.g. off Africa and East Asia), or where the aerosols
1007 are believed to have strong absorption (e.g. off Southern Africa or southern Asia). Since
1008 the current suite of C005 aerosol models are spherical and weakly absorbing, it was
1009 consistent that the comparison would be better over the open ocean or downwind of the
1010 developed nations (e.g., off the US East Coast). In general the comparisons were similar
1011 for both Terra and Aqua.

1012

1013 In response to community needs and concerns, we calculated EU for size parameters, in
1014 particular the Ångström exponent and fine AOD. Globally, we found that Ångström
1015 exponent over land (α_L) and ocean (α_O) agreed with AERONET values to within ± 0.45
1016 and ± 0.3 , respectively. Due to the lack of the full range of aerosol model choices, the
1017 dynamic range of MODIS's α_L (over land) was insufficient to capture the true range
1018 observed by AERONET. MODIS's Angstrom exponent also was not well correlated
1019 with AERONET values over land ($R \sim 0.55$), suggesting that it cannot be considered a
1020 quantitative product, globally. There are regions, however, such as the eastern United
1021 States (e.g. GSFC site), where α_L displays some skill. Over ocean, α_O showed good
1022 correlation ($R \sim 0.8$), although with slope less than unity. We believe the over ocean
1023 discrepancies are due to a combination of too little absorption and too much sphericity in
1024 the models to accurately retrieve large amounts of very small (absorbing biomass
1025 burning) and large (dust) aerosols. Analyses of retrieved fine AOD over both land and

1026 ocean showed that their discrepancies were consistent with those demonstrated by the
1027 Ångström exponent comparisons.
1028
1029 Finally, we derived the fraction of expected uncertainty (FEU) to characterize how the
1030 comparison of total AOD may be changing over time. From MODIS/AERONET
1031 comparisons at several long-term sites, we found that compared to AERONET, there is
1032 no systematic change in the MODIS data over time over ocean for either MODIS sensor.
1033 Although one must remember that MODIS data and AERONET observations are not
1034 exactly collocated over the ocean, there is some evidence that Terra has been slightly
1035 overestimating, whereas Aqua may have been slightly underestimating the true AOD
1036 over ocean. Over land, Aqua comparisons do not show a change over time, and the mean
1037 values from both AERONET and MODIS are comparable. However, there is a
1038 statistically significant change in the MODIS/AERONET comparison for Terra over
1039 land, from MODIS overestimating early in the mission, to underestimating in the later
1040 period. We believe the issue is a degradation of Terra's optical response in the 0.47 μm
1041 channel (used in the land algorithm only) that results in very small errors to the sensor's
1042 calibration over time. The calibration issues should be updated in a future reprocessing
1043 of MODIS data.

1044

1045 In this paper, we have assessed the performance of the MODIS aerosol (AOD and size
1046 parameters) compared to AERONET observations. We have not attempted to
1047 characterize the MODIS data that is not collocated with AERONET. However, we now
1048 have defined a quantitative EU for some of the MODIS products. By learning where and

1049 when the MODIS algorithm appears to fall short of meeting expectations, we are
1050 performing necessary steps for future improvements. We now have a solid base in which
1051 to develop algorithms that may be used for deriving future collections of MODIS data.

1052

1053

1054 **Acknowledgements: We are deeply grateful to Wayne Newcomb, who was a vital**
1055 **member of the AERONET team from the genesis of the project until he sadly passed**
1056 **away in December 2008. We miss him, his dedication to details and his ability to**
1057 **talk a novice through a Cimel installation via a phone link across countless miles**
1058 **and time zones. Without Wayne and the many AERONET Principal Investigators**
1059 **and site managers, the data base used in this study would not be possible. This**
1060 **work has been funded by NASA research announcement NNH06ZDA001N-EOS,**
1061 managed by Hal Maring.

1062

1063 **References**

1064

1065 Ackerman, S.A., K.I. Strabala, W.P. Menzel, R.A. Frey, C.C. Moeller and L.E. Gumley,
1066 1998: Discriminating clear sky from clouds with MODIS. *J. Geophys. Res.*, **103**,
1067 32139-32140.

1068 Al-Saadi, J., J. Szykman, R. B. Pierce, C. Kittaka, D. Neil, D. A. Chu, L. Remer, L.
1069 Gumley, E. Prins, L. Weinstock, C. MacDonald, R. Wayland, F. Dimmick and J.
1070 Fishman, 2005: Improving National Air Quality Forecasts with Satellite Aerosol
1071 Observations. *Bull. Am. Met. Soc.* 86, 1249-1261.

1072

1073 Anderson T.L., R.J Charlson, D.M. Winker, J.A. Ogren and K. Holmen, 2003:
1074 Mesoscale variations of tropospheric aerosols, . *J. Atmos. Sci.*, **60**, 119-136.

1075

1076 Franz, B. A. S. W. Bailey, P. J. Werdell, and C. R. McClain, "Sensor-independent
1077 approach to the vicarious calibration of satellite ocean color radiometry," *Appl.*
1078 *Opt.* 46, 5068-5082 (2007)

1079

1080 Chu, D. A., Y. J. Kaufman, C. Ichoku, L. A. Remer, D. Tanre, and B. N. Holben, 2002:
1081 Validation of MODIS aerosol optical depth retrieval over land. *Geophys. Res.*
1082 *Lett.*, **29**, doi: 10.1029/2001GLO13205.
1083
1084 Dubovik, O. and M. D. King, 2000: A flexible inversion algorithm for retrieval of aerosol
1085 optical properties from Sun and sky radiance measurements," *J. Geophys. Res.*,
1086 **105**, 20 673-20 696.
1087
1088 Dubovik, O., B.N.Holben, T.F.Eck, A.Smirnov, Y.J.Kaufman, M.D.King, D.Tanre, and
1089 I.Slutsker, 2002: Variability of absorption and optical properties of key aerosol
1090 types observed in worldwide locations, *J.Atm.Sci.*, **59**, 590-608 .
1091
1092 Eck, T.F., B.N.Holben, J.S.Reid, O.Dubovik, A.Smirnov, N.T.O'Neill, I.Slutsker, and
1093 S.Kinne, 1999: Wavelength dependence of the optical depth of biomass burning,
1094 urban and desert dust aerosols, *J. Geophys. Res.*, **104**, 31 333-31 350.
1095
1096 Franz, B. A. S. W. Bailey, P. J. Werdell, and C. R. McClain, 2007: Sensor-independent
1097 approach to the vicarious calibration of satellite ocean color radiometry, *Appl.*
1098 *Opt.* **46**, 5068-5082.
1099
1100 Gao, B.-C., Y.J. Kaufman, D. Tanré and R.-R. Li, 2002: Distinguishing tropospheric
1101 aerosols from thin cirrus clouds for improved aerosol retrievals using the ratio of
1102 1.38- μm and 1.24- μm channels. *Geophys. Res. Lett.*, **29**, 1890,
1103 doi:10.1029/2002GL015475.
1104
1105 Holben, B.N., T.F. Eck, I. Slutsker, D. Tanré, J.P. Buis, A. Setzer, E. Vermote, J.A.
1106 Reagan, Y.J. Kaufman, T. Nakajima, F. Lavenu, I. Jankowiak and A. Smirnov,
1107 1998: AERONET--A federated instrument network and data archive for aerosol
1108 characterization. *Rem. Sens. Environ.*, **66**, 1-16.
1109
1110 Hubanks, P.A., 2007: MODIS Atmosphere QA Plan for Collection 005 Deep Blue
1111 Aerosol Update Version 3.5, available from [http://modis-](http://modis-atmos.gsfc.nasa.gov/reference_atbd.php)
1112 [atmos.gsfc.nasa.gov/reference_atbd.php](http://modis-atmos.gsfc.nasa.gov/reference_atbd.php), 61 pps.
1113 Hsu, N. C., S. C. Tsay, M. D. King, and J. R. Herman, 2004: Aerosol properties over
1114 bright-reflecting source regions. *IEEE Trans. Geosci. Remote Sens.*, **42**, 557-569.
1115
1116 Ichoku, C., D.A. Chu, S. Mattoo, Y.J. Kaufman, L.A. Remer, D. Tanré, I. Slutsker and
1117 B.N. Holben, 2002: A spatio-temporal approach for global validation and analysis
1118 of MODIS aerosol products. *Geophys. Res. Lett.*, **29**, 10.1029/2001GL013206.
1119
1120 Ichoku, C., L. A. Remer, Y. J. Kaufman, R. Levy, D. A. Chu, D. Tanre, and B. N.
1121 Holben, 2003: MODIS observation of aerosols and estimation of aerosol radiative
1122 forcing over southern Africa during SAFARI 2000. *J. Geophys. Res.*, **108** (D13),
1123 8499, doi: 10.1029/2002JD002366.
1124

1125 Ichoku, C., L. A. Remer, and T. F. Eck, 2005: Quantitative evaluation and
1126 intercomparison of morning and afternoon MODIS aerosol measurements from
1127 Terra and Aqua. *J. Geophys. Res.* **110**, D10S03, doi: 10.1029/2004JD004987.
1128

1129 IPCC, 2007: Climate Change 2007: The Physical Science Basis. Contribution of Working
1130 Group I to the Fourth Assessment Report of the Intergovernmental Panel on
1131 Climate Change [Solomon, S., D. Qin, M. Manning, Z. Chen, M. Marquis, K.B.
1132 Averyt, M. Tignor and H.L. Miller (eds.)]. Cambridge University Press,
1133 Cambridge, United Kingdom and New York, NY, USA, 996 pp.
1134

1135 Jethva, H., S.K. Satheesh and J. Srinivasan, 2007: Assessment of second-generation
1136 MODIS aerosol retrieval (Collection 005) at Kanpur, India. *Geophys. Res. Lett.*,
1137 **34**, L19802, doi:10.1029/2007GL029647.
1138

1139 Kaufman, Y. J., and C. Sendra, 1988: Algorithm for atmospheric corrections of visible
1140 and Near IR satellite imagery. *Int. J. Rem. Sens.*, **9**, 1357-1381.
1141

1142 Kaufman, Y. J., D. Tanre, L. Remer, E. Vermote, A. Chu, and B. N. Holben, 1997:
1143 Operational remote sensing of tropospheric aerosol over land from EOS Moderate
1144 Resolution Imaging Spectroradiometer. *J. Geophys. Res. (Atmos.)*, **102**, 17051-
1145 17067.
1146

1147 Kaufman, Y. J., O. Boucher, D. Tanre, M. Chin, L. A. Remer, and T. Takemura, 2005:
1148 Aerosol anthropogenic component estimated from satellite data. *Geophys. Res.*
1149 *Lett.* **32**, L17804, doi:10/1029/2005GL023125.
1150

1151 Kleidman, R.G., N.T. O'Neill, L.A. Remer, Y.J. Kaufman, T.F. Eck, D. Tanré, and B.N.
1152 Holben 2005: Comparison of moderate resolution Imaging spectroradiometer
1153 (MODIS) and aerosol robotic network (AERONET) remote-sensing retrievals of
1154 aerosol fine mode fraction over ocean. *J. Geophys. Res.*, **110** D22205,
1155 doi:10.1029/2005JD005760.
1156

1157 Levy, R.C., L.A. Remer, D. Tanré, Y.J. Kaufman, C. Ichoku, B.N. Holben, J.M.
1158 Livingston, P.B. Russell and H. Maring, 2003: Evaluation of the MODIS
1159 retrievals of dust aerosol over the ocean during PRIDE. *J. Geophys. Res.*, **108**
1160 (D14), 10.1029/2002JD002460
1161

1162 Levy, R. C., L. A. Remer, J. V. Martins, Y. J. Kaufman, A. Plana-Fattori, J. Redemann,
1163 P. B. Russell, and B. Wenny, 2005: Evaluation of the MODIS aerosol retrievals
1164 over ocean and land during CLAMS. *J. Atmos. Sci.*, **62**, 974-992.
1165

1166 Levy, R. C., L. A. Remer, and O. Dubovik, 2007a: Global aerosol optical properties and
1167 application to MODIS aerosol retrieval over land. *J. Geophys. Res.*, **112**, D13210,
1168 doi:10.1029/2006JD007815.
1169

1170 Levy, R. C., L. Remer, S. Mattoo, E. Vermote, and Y. J. Kaufman, 2007a: Second-
1171 generation algorithm for retrieving aerosol properties over land from MODIS
1172 spectral reflectance. *J. Geophys. Res.*, 112, D13211, doi:10.1029/2006JD007811.
1173

1174 Levy, R.C., G. G. Leptoukh, R. Kahn, V. Zubko, A. Gopalan and L.A. Remer, 2009b: A
1175 critical look at deriving monthly aerosol optical depth from satellite data, , *IEEE*
1176 *Trans. Geosci. Remote Sens.*, in press.
1177

1178 Levy, R.C., L.A. Remer, D. Tanré, Y.J. Kaufman and S. Mattoo, 2009: Algorithm for
1179 Remote Sensing of Tropospheric Aerosol from MODIS: Collection 005 –
1180 Revision 2. Algorithm Theoretical Basis Document available at [http:// modis-](http://modis-atmos.gsfc.nasa.gov/reference_atbd.php)
1181 [atmos.gsfc.nasa.gov/reference_atbd.php](http://modis-atmos.gsfc.nasa.gov/reference_atbd.php).
1182
1183

1184 Li, R.-R., Y.J. Kaufman, B.-C. Gao and C.O. Davis, 2003: Remote sensing of suspended
1185 sediments and shallow coastal waters. *IEEE TGARS*, **41**, 559-566.
1186

1187 Martins, J.V., D. Tanré, L.A. Remer, Y.J. Kaufman, S. Mattoo and R. Levy, 2002:
1188 MODIS Cloud screening for remote sensing of aerosol over oceans using spatial
1189 variability. *Geophys. Res. Lett.*, **29**, 10.1029/2001GL013252.
1190

1191 Mi, W., Z. Li, X. Xia, B. Holben, R. Levy, F. Zhao, H. Chen, and M. Cribb, 2007:
1192 Evaluation of the Moderate Resolution Imaging Spectroradiometer aerosol
1193 products at two Aerosol Robotic Network stations in China, *J. Geophys. Res.*,
1194 **112**, D22S08, doi:10.1029/2007JD008474.
1195

1196 O'Neill, N.T., T.F.Eck, , A.Smirnov, B.N.Holben, and S.Thulasiraman, Spectral
1197 discrimination of coarse and fine mode optical deph, *J. Geophys. Res.*, 108(D17),
1198 4559, doi:10.1029/2002JD002975, 2003.
1199

1200 Redemann, J., B. Schmid, J. A. Eilers, R. Kahn, R. C. Levy, P. B. Russell, J. M.
1201 Livingston, P. V. Hobbs, W. L. Smith, and B. N. Holben, 2005: Suborbital
1202 measurements of spectral aerosol optical depth and its variability at subsatellite
1203 grid scales in support of CLAMS 2001. *J. Atmos. Sci.*, **62**, No. 4, 993-1007.
1204

1205 Redemann, J., Q. Zhang, J. Livingston, P. Russell, Y. Shinozuka, A. Clarke, R. Johnson,
1206 and R. Levy, 2009: Testing aerosol properties in MODIS (MOD35/MYD35)
1207 Collection 4 and 5 using airborne sunphotometer observations in INTEX-
1208 B/MILAGRO, *Atmos. Chem . Phys.*, in preparation.
1209

1210 Redemann, J., Q. Zhang, B. Schmid, P. B. Russell, J. M. Livingston, H. Jonsson, and L.
1211 A. Remer, 2006: Assessment of MODIS-derived visible and near-IR aerosol
1212 optical properties and their spatial variability in the presence of mineral dust.
1213 *Geophys. Res. Lett.*, **33**, L18814, doi:10.1029/2006GL026626.
1214

1215 Remer, L.A., D. Tanré, Y.J. Kaufman, C. Ichoku, S. Mattoo, R. Levy, D.A. Chu, B.N.
1216 Holben, O. Dubovik, A. Smirnov, J.V. Martins, R.-R. Li and Z. Ahmad, 2002:
1217 Validation of MODIS aerosol retrieval over ocean. *Geophys. Res. Lett.*, **29**,
1218 10.1029/2001GL013204.
1219
1220 Remer, L. A., Y. J. Kaufman, D. Tanre, S. Mattoo, D. A. Chu, J. V. Martins, R. R. Li, C.
1221 Ichoku, R. C. Levy, R. G. Kleidman, T. F. Eck, E. Vermote, and B. N. Holben,
1222 2005: The MODIS aerosol algorithm, products and validation. *J. Atmos. Sci.*, **62**,
1223 947-973.
1224
1225 Remer L. A., et al. 2008: Global aerosol climatology from the MODIS satellite sensors, *J.*
1226 *Geophys. Res.*, **113**, D14S07, doi:10.1029/2007JD009661.
1227
1228 Smirnov A., B.N.Holben, T.F.Eck, O.Dubovik, and I.Slutsker, 2000: Cloud screening and
1229 quality control algorithms for the AERONET database, *Rem.Sens.Env.*, **73**, 337-
1230 349.
1231
1232 Smirnov, A., B.N.Holben, Y.J.Kaufman, O.Dubovik, T.F.Eck, I.Slutsker, C.Pietras, and
1233 R.Halthore, 2002: Optical Properties of Atmospheric Aerosol in Maritime
1234 Environments, *J.Atm.Sci.*, **59**, 501-523.
1235
1236 Tanré, D., M. Herman, and Y. Kaufman, 1996: Information on the aerosol size
1237 distribution contained in the solar reflected spectral radiances. *J. Geophys. Res.*,
1238 **101**, 19043-19060.
1239
1240 Tanré, D., Y. J. Kaufman, M. Herman, and S. Mattoo, 1997: Remote sensing of aerosol
1241 properties over oceans using the MODIS/EOS spectral radiances. *J. Geophys.*
1242 *Res. (Atmos.)*, **102**, 16971-16988.
1243
1244 Yu, H., Y. J. Kaufman, M. Chin, G. Feingold, L. Remer, T. Anderson, Y. Balkanski, N.
1245 Bellouin, O. Boucher, S. Christopher, P. DeCola, R. Kahn, D. Koch, N. Loeb, M.
1246 S. Reddy, M. Schulz, T. Takemura, and M. Zhou, 2006: A review of
1247 measurement-based assessments of aerosol direct radiative effect and forcing.
1248 *Atmos. Chem. Phys.*, **6**, 613-666.
1249
1250 Xiong, X., J. Sun, W. Barnes, V. Salomonson, J. Esposito, H. Erives, and B. Guenther,
1251 2007: Multiyear On-Orbit Calibration and Performance of Terra MODIS
1252 Reflective Solar Bands, *IEEE Trans. Geosci. Remote Sens.*, 45(4), 879-889.
1253
1254

Figures

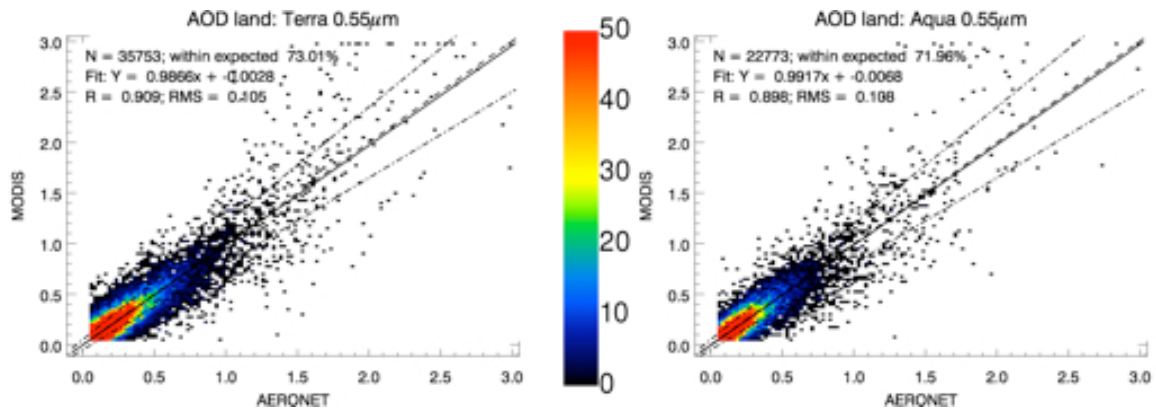


Figure 1: MODIS C005 AOD retrievals over dark land (QC=3) at 550 nm as a function of AERONET observations collocated in space and time, for the entire mission of Terra (left) and Aqua (right). The data were sorted according to ordered pairs (AERONET, MODIS) of AOD in 0.025 intervals, so that color represents the number of cases (colorbar) having that particular ordered pair value. The dashed, dotted and solid lines are the 1-1 line, EU for land AOD ($\pm 0.05 \pm 0.15\tau$), and the linear regression of the pre-sorted scatterplot, respectively. At the top of the plot is text that describes: the number of collocations (N), the percent within expected uncertainty, the regression curve, correlation (R), and the RMS error of the fit.

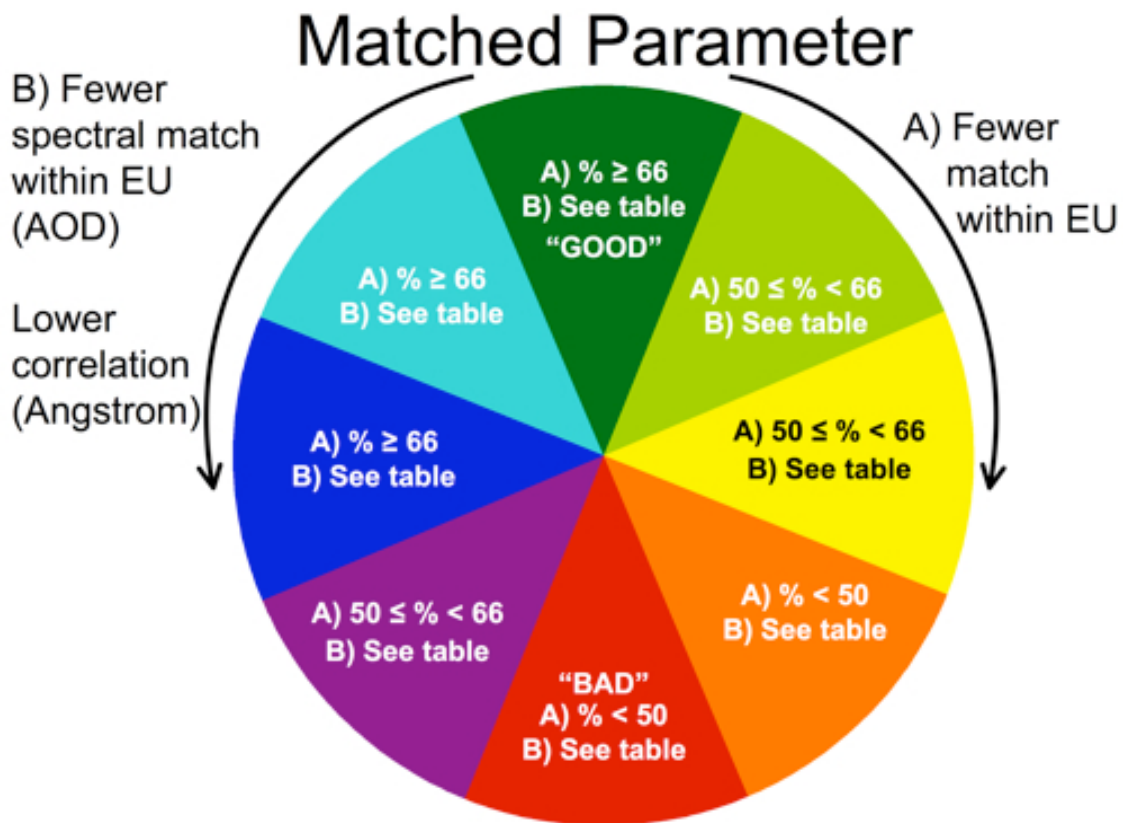


Figure 2: Guide to interpreting seasonal, site-by-site maps of MODIS/AERONET matching quality of certain derived parameters (Figs XXXXX). The color indicates the joint results from of two conditional tests, where each test's result may be described subjectively (e.g., good, marginal, bad). For all parameters, test "A" considers how many of the MODIS/AERONET pairs match within the EU defined for the given parameter, such that the case where $>66\%$ match is denoted as "good" and $<50\%$ match is "bad." The details of test "B" depend on which parameter is being matched. The green color represents a good overall match, meaning that the result of both tests A and test B is "good". A red color represents the case that the result from both tests is "bad." Circling from green to red counterclockwise (colder colors) represents sites with better results from test A than test B, whereas going clockwise (warmer colors) represents sites with better results from test B than test A. Details of the tests for given parameters is given in Table 2.

Terra; Summer: JJA

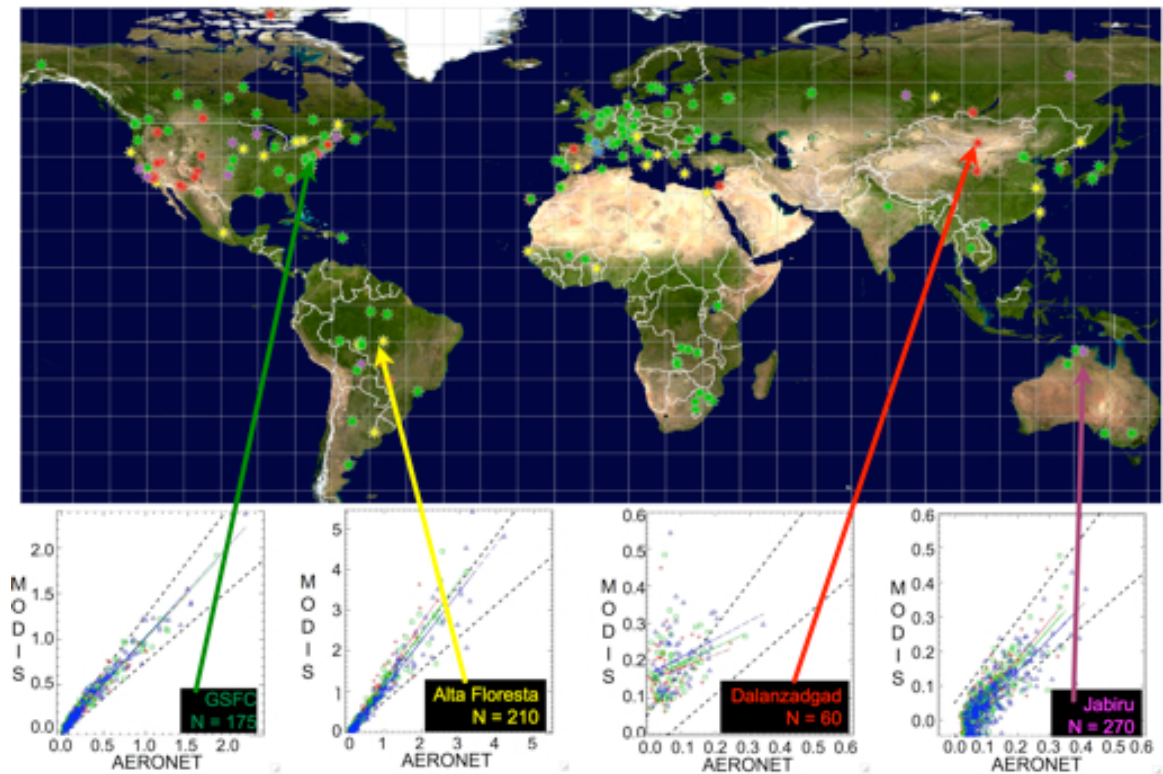


Figure 3: “Quality” of Terra-MODIS/AERONET comparisons of total and spectral AOD over land at each site, from Terra, during the summer. The color at each represents the quality of the comparison (Fig. 2 and Table 2). The comparisons of spectral AOD (different symbols: blue - 0.47 μm , green - 0.55 μm , red - 0.66 μm) at four sites are plotted, including: GSFC (38N, 76W), Alta Floresta (9S, 56W), Dalanzadgad (43N, 104E) and Jabiru (12S, 132E). The dotted lines for each scatterplot are the expected uncertainty ($\pm 0.05 \pm 0.15\tau$) over land.

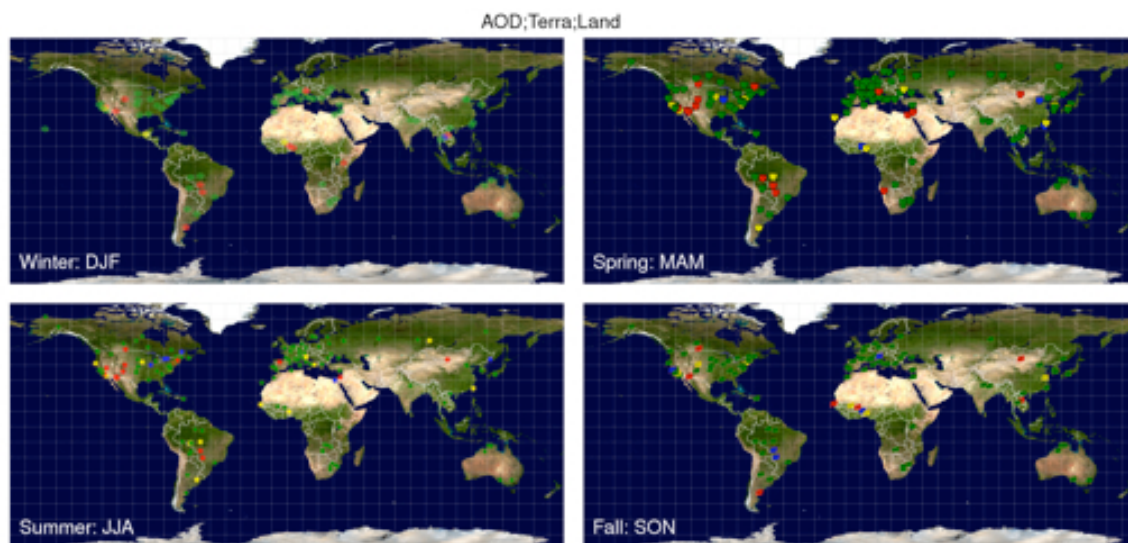


Figure 4: “Quality” of Terra-MODIS/AERONET comparisons of total and spectral AOD over land at each site, separated by season. Icons (Snowflake, Tulip, Sunshine, Leaf) represent each season and colors represent the quality of the comparison (Fig. 2 and Table 2). Note that not all sites have valid collocations for all seasons.

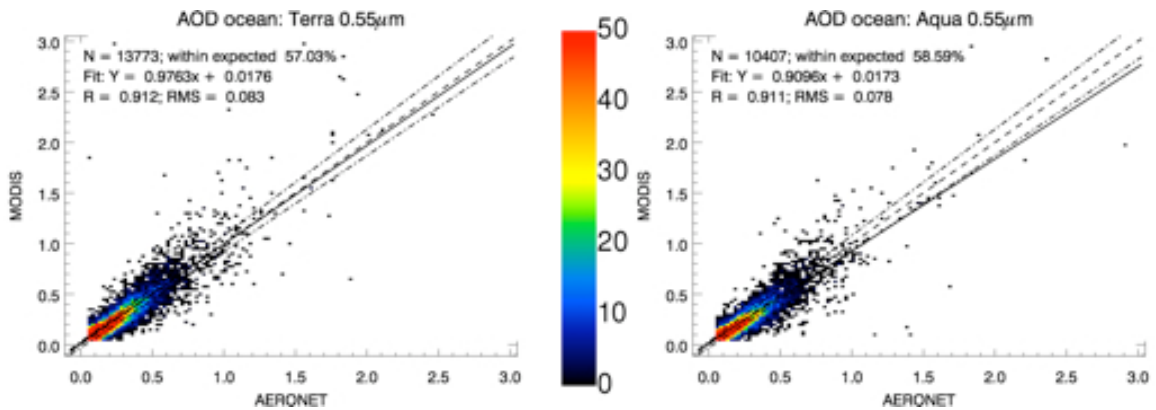


Figure 5: Same as Fig. 1 but for MODIS C005 AOD retrievals over ocean ($QC \geq 1$). Here the dotted lines envelope the predefined EU for ocean AOD ($\pm 0.03 \pm 0.05\tau$).

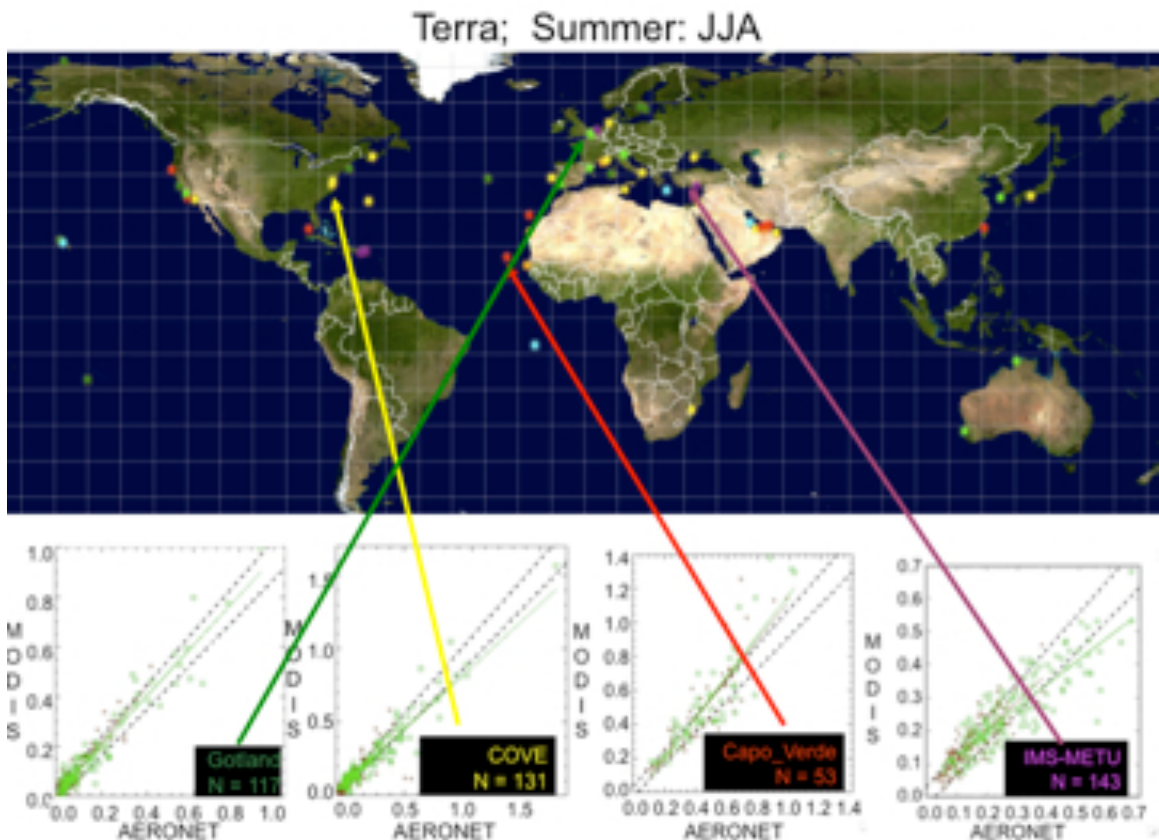


Figure 6: “Quality” of Terra-MODIS/AERONET comparisons of total and spectral AOD over ocean at each site, from Terra, during the summer. The color at each represents the quality of the comparison (Fig. 2 and Table 2). The comparisons of spectral AOD (different symbols: green - $0.55 \mu\text{m}$, brown - $0.86 \mu\text{m}$) at four sites are plotted, including: Gotland ($58\text{N}, 19\text{E}$), COVE ($37\text{N}, 76\text{W}$), Capo_Verde ($17\text{N}, 23\text{W}$) and IMS-METU ($37\text{N}, 34\text{E}$). The dotted lines for each scatterplot are the EU ($\pm(0.04+0.05\tau)$) for ocean AOD.

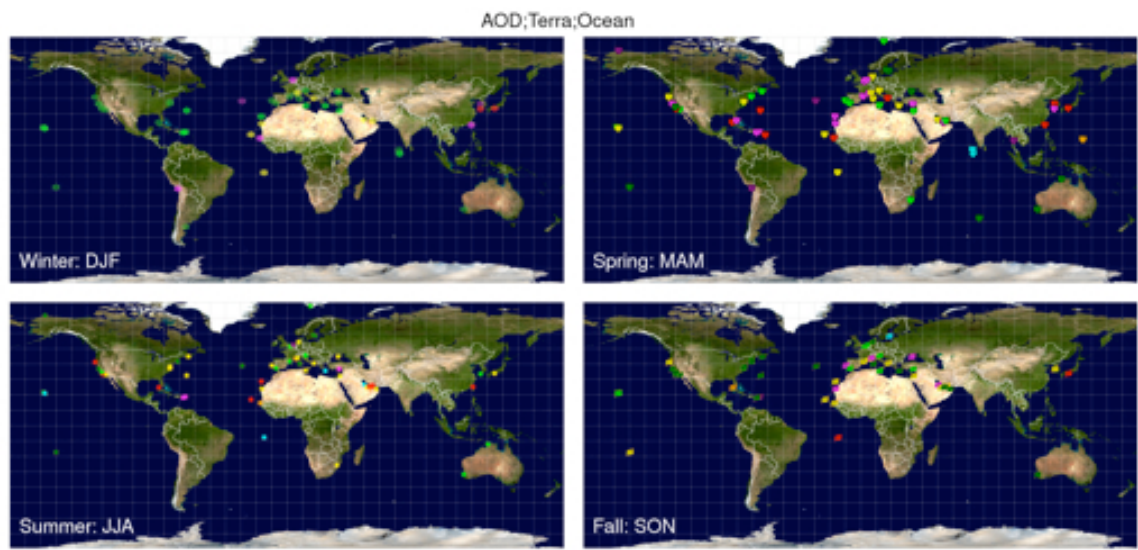


Figure 7: Same as Fig. 4 but for total and spectral AOD over ocean (see Table 2 for details).

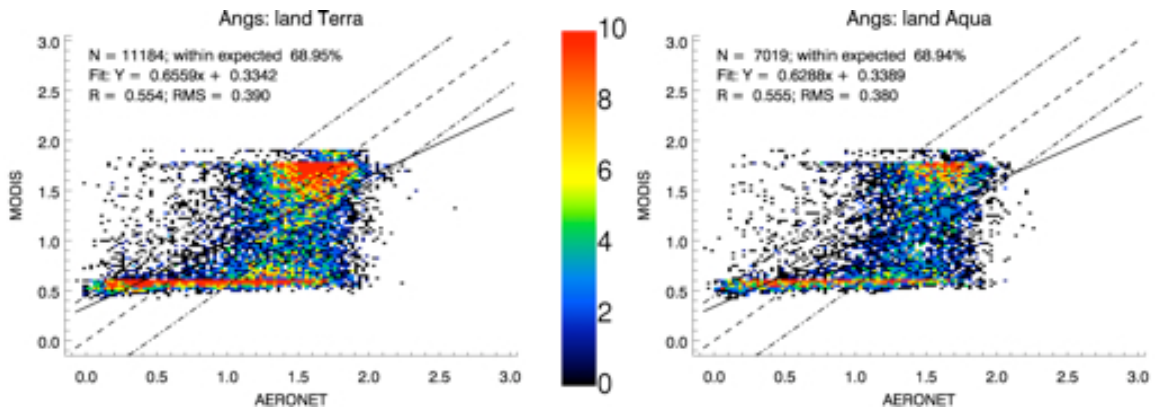


Figure 8: Same as Fig. 1 but for MODIS C005 Ångstrom exponent retrievals (0.47/0.66 μm) over dark land ($\tau > 0.2$; QC=3). The dotted lines envelope the EU, (± 0.45).

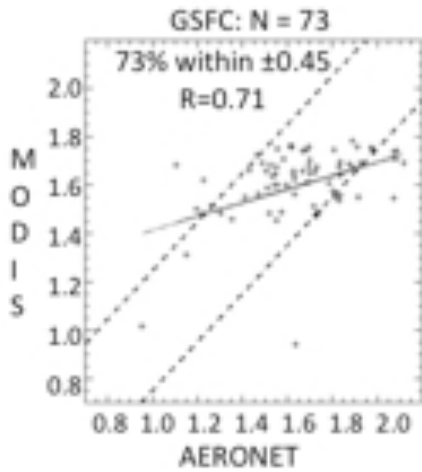


Figure 9: Ångstrom exponent over land at GSFC during the summer for Terra compared with AERONET. The dotted lines are the EU (± 0.45)

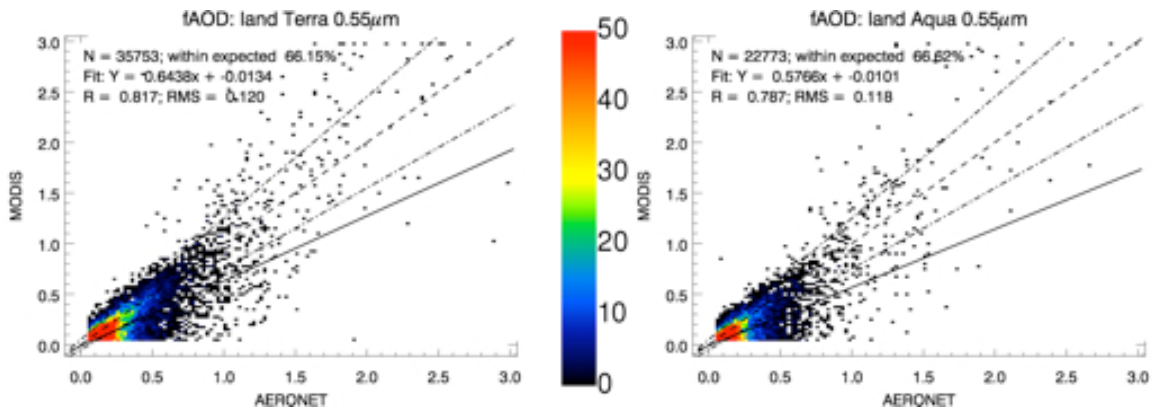


Figure 10: Same as Fig. 1 but for MODIS C005 fAOD retrievals over dark land (QC=3) at 550 nm. The dotted lines envelope the EU, estimated as $(\pm 0.05 \pm 0.20\tau)$.

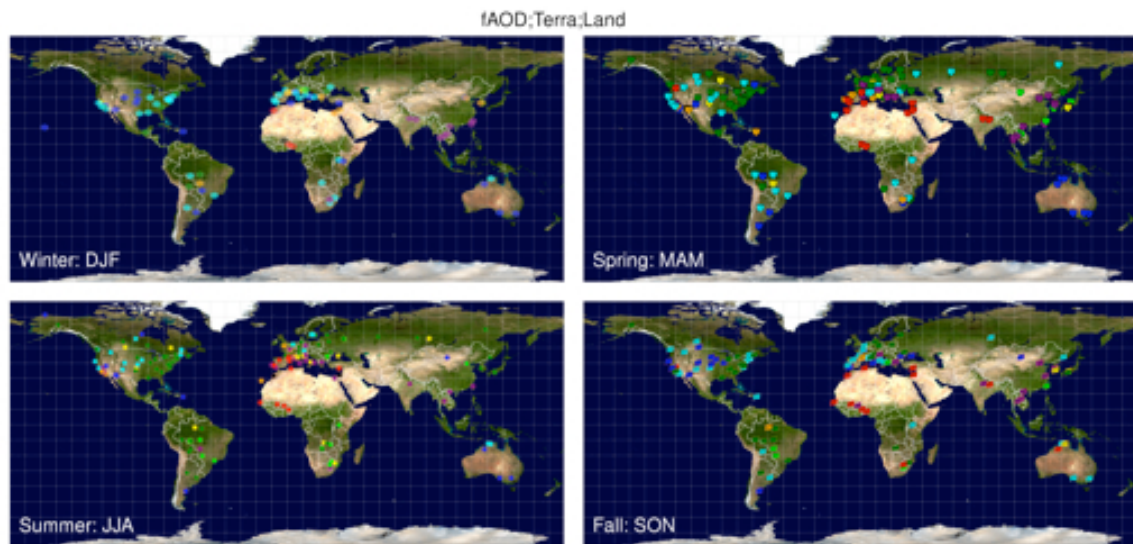


Figure 11: Same as Fig. 4 but for assessing fAOD over land (see Table 2 for details).

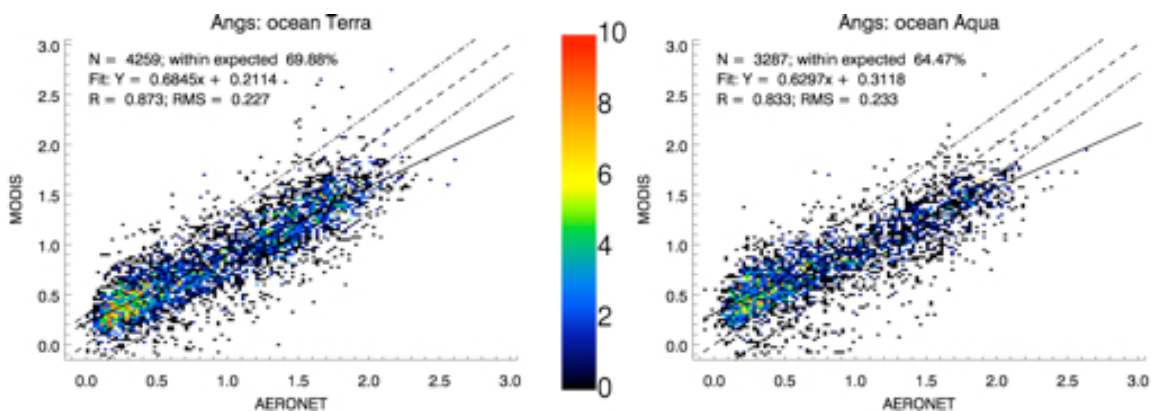


Figure 12: Same as Fig 1, but for MODIS C005 Ångstrom exponent retrievals ($0.47/0.87 \mu\text{m}$) over water ($\tau > 0.15$; $QC \geq 1$). The dotted lines represent EU of (± 0.3).

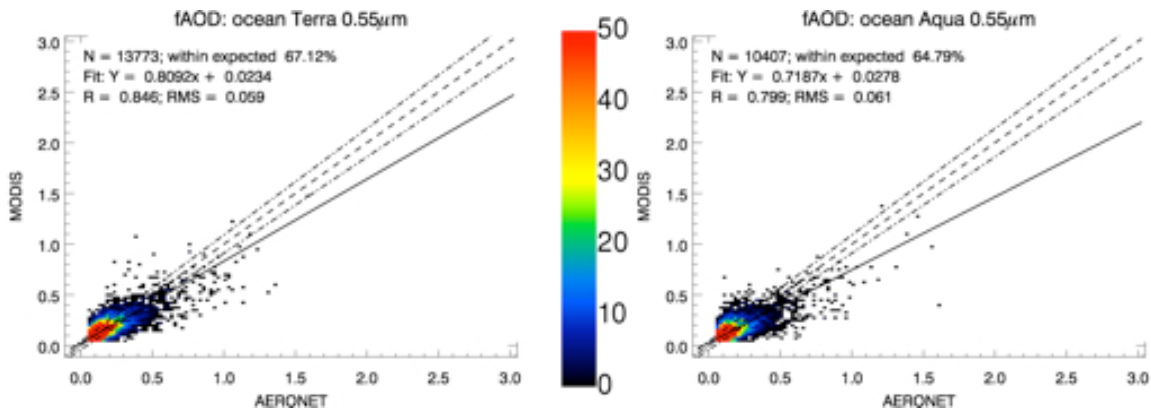


Figure 13: Same as Fig. 1, but for MODIS C005 fAOD retrievals over water ($QC \geq 1$) at 550 nm. The dotted lines represent EU of ($\pm 0.05 \pm 0.05\tau$).

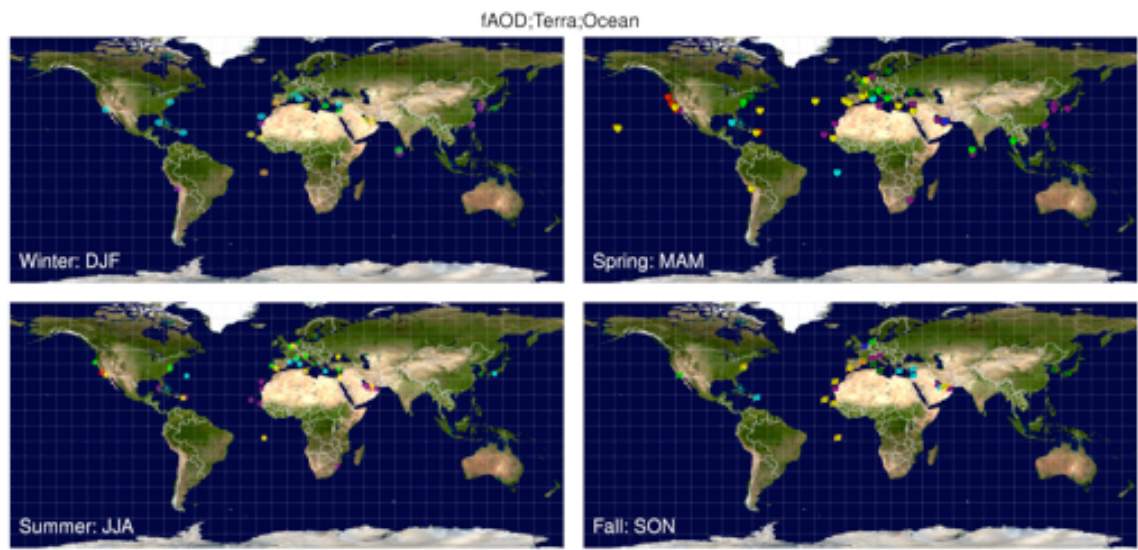


Figure 14: Same as Fig. 4 but for assessing fAOD over ocean (see Table 2 for details).

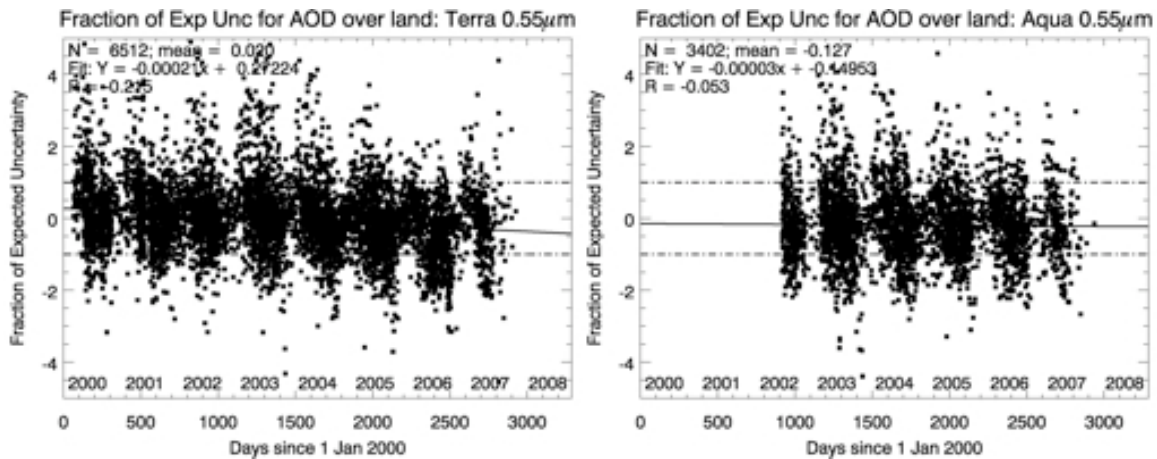


Figure 15: Time series of “fraction of expected uncertainty” (FEU) of MODIS C005 AOD (550 nm) compared to long-term AERONET, over dark land, for Terra (left) and Aqua (right). Points between the dashed lines (± 1) are cases where MODIS matches AERONET within EU over land ($\pm 0.05 \pm 0.15\tau$). The solid line is the linear regression. At the top of the plot is text that describes: the number of collocations (N), the regression equation and correlation (R).

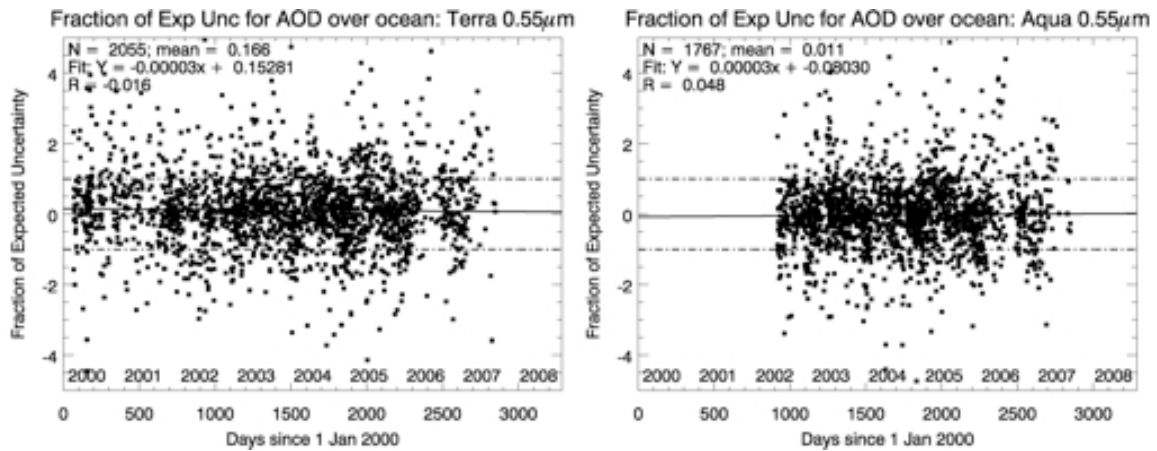


Figure 16: Same as Fig 13, but for MODIS C005 AOD over water. The EU is ($\pm 0.04 \pm 0.05\tau$).